V．研究成果の刊行物・別刷

Available online at www.sciencedirect.com
SCIENCE DIRECT®
Cytokine & Growth Factor Reviews xxx (2005) xxx–xxx
Cytokine Growth Factor Reviews
www.elsevier.com/locate/cytogfr

BMP antagonists: Their roles in development and involvement in pathophysiology

Motoko Yanagita *

COE Formation for Genomic Analysis of Disease Model Animals with Multiple Genetic Alterations, Graduate School of Medicine, Kyoto University, Kyoto 606-8507, Japan

Abstract

Bone morphogenetic proteins (BMPs) are phylogenetically conserved signaling molecules that belong to the transforming growth factor (TGF)-β superfamily, and are involved in the cascades of body patterning and morphogenesis. The activities of BMPs are precisely regulated by certain classes of molecules that are recently recognized as BMP antagonists. BMP antagonists function through direct association with BMPs, thus prohibiting BMPs from binding their cognate receptors. In this review, the classification and functions of BMP antagonists will be discussed, especially focusing on the new family of tissue-specific BMP antagonists composed of uterine sensitization-associated gene 1 (USAG-1) and sclerostin.

Keywords: USAG-1; Wise; Ectodin; Sclerostin; Cystine-knot

1. Introduction

Bone morphogenetic proteins (BMPs) are phylogenetically conserved signaling molecules that belong to the transforming growth factor (TGF)-β superfamily [1–4]. Although these proteins were first identified by their capacity to promote endochondral bone formation [5–7], they are involved in the cascades of body patterning and morphogenesis [8]. Furthermore, BMPs play important roles after birth in pathophysiology of several diseases including osteoporosis [9], arthritis [5], kidney diseases [10–12], pulmonary hypertension [13,14], cerebrovascular diseases [15] and cancer [16].

In addition to the tissue-specific expression of BMPs and their cell surface receptors, BMP signaling is precisely regulated by certain classes of molecules that are recently recognized as BMP antagonists [1–3,17]. These BMP antagonists function through direct association with BMPs, thus prohibiting BMPs from binding their cognate receptors. The interplay between BMP and their antagonists governs developmental and cellular processes as diverse as establishment of the embryonic dorsal–ventral axis [18], induction of neural tissue [19], formation of joints in the skeletal system [5] and neurogenesis in the adult brain [20].

In this review, the classification and functions of BMP antagonists will be discussed, especially focusing on the new family of BMP antagonists composed of uterine sensitization-associated gene 1 (USAG-1) and sclerostin.

2. Classification of BMP antagonists

Since chordin and noggin, secretory proteins expressed in the Spemann organizer of *Xenopus* embryos, are elucidated to inhibit BMP signaling through direct binding [1–3,5] (see Sections 6 and 7), number of proteins are documented as members of the BMP antagonists. BMP antagonists have a secretory signal peptide and cysteine arrangement consistent with the formation of the cystine-knot structure and represent a subfamily of cystine-knot superfamily, which comprises of many homodimeric and heterodimeric proteins such as TGF-β, growth differentiation factors (GDFs), gonadotropins, and platelet-derived growth factors, and BMPs [21]. Recently, Avsian-Kretchmer et al. classified BMP antagonists into three subfamilies based on the size of

* Tel.: +81 75 751 3670; fax: +81 75 751 3203.
E-mail address: motoy@kuhp.kyoto-u.ac.jp.

1359-6101/$ – see front matter © 2005 Elsevier Ltd. All rights reserved.
doi:10.1016/j.cytogfr.2005.02.007

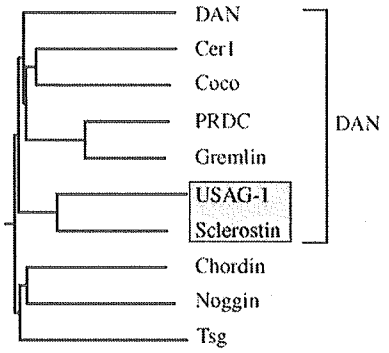

Fig. 1. Phylogenetic tree of BMP antagonists. Phylogenetic tree of human BMP antagonists based on the overall amino acid sequence similarity of representative members from each subfamily. The GenomeNet server at http://www.genome.jp/ was used for phylogenetic tree construction.

the cystine-knot [17]: the DAN family (eight-membered ring) [22–24]; twisted gastrulation (nine-membered ring) [25–28]; and chordin and noggin (10-membered ring) [29–31]. They further divided the DAN family into four subgroups based on a conserved arrangement of additional cysteine residues outside of the cystine-knots: [1] PRDC [32] and gremlin[22,33,34]; [2] coco [35] and Cerl [23]; homologue of *Xenopus* Cerberus; [3] Dan [36,37]; and [4] USAG-1 [38,39] and sclerostin [40–42]. This subdivision is almost consistent with the phylogenic tree, based on the overall amino acid sequence similarity shown in Fig. 1.

USAG-1 and sclerostin are newly defined BMP antagonists abundantly expressed in the kidneys and bones, respectively. The discovery, function, and expression of these unique BMP antagonists will be discussed later in detail (see Sections 3 and 4). In addition to the entire amino acids sequence similarity, there are several evidences to support the idea that USAG-1 and sclerostin form a distinct family of BMP antagonists. One reason is the evolutionary origin of the genes; genes for USAG-1 and sclerostin are missing in fly and nematode; however, a single ortholog for both USAG-1 and sclerostin was found in *Fugu rubripes* and *Ciona intestinalis* [17]. Furthermore, exon–intron arrangements of all orthologous genes for USAG-1 and sclerostin are highly conserved [17]. Another reason is that USAG-1 and sclerostin are secreted as monomers [38,40], while many other BMP antagonists form dimers [30]. This result is consistent with the findings that many BMP antagonists possess extra cysteine residues that could allow the formation of homodimers, which are missing in USAG-1 and sclerostin [17].

3. USAG-1

3.1. BMP-7 and kidney diseases

BMP-7, also known as osteogenic protein-1 (OP-1), is a 35 kDa homodimeric protein, and the kidney is the major site of BMP-7 synthesis [43–46] during embryogenesis as well as postnatal development. Its genetic deletion in mice leads to severe impairment of kidney development resulting in perinatal death [47,48]. Expression of BMP-7 in adult kidney is confined to distal collecting tubules and podocytes of glomeruli [49], and the expression decreases in several kidney disease models [50–54]. Recently, several reports indicate that the administration of recombinant BMP-7 inhibits the progression of chronic kidney disease in animal models [51–53,55–59]; BMP-7 inhibits epithelial-to-mesenchymal transition (EMT) of tubular epithelial cells, and reduces the fibrosis of interstitium [59]. However, the regulatory mechanism of the action of BMP-7 in the kidney has not been elucidated.

3.2. Discovery of USAG-1

Through a genome-wide search for kidney-specific human transcripts, our group found a novel gene, which encodes a secretory protein with a signal peptide and cysteine-rich domain [38]. The rat orthologue of the gene was previously reported as a gene of unknown function that was preferentially expressed in sensitized endometrium of rat uterus, termed uterine sensitization-associated gene-1 (USAG-1) [39]. Amino acid sequences encoded in the rat and mouse cDNAs are 97% and 98% identical to the human sequence respectively, indicating high degrees of sequence conservation.

Domain search predicted this protein to be a member of the cystine-knot superfamily, with signal peptide of 23 amino acids [38]. Homology search revealed that USAG-1 has significant amino acid identities (38%) to sclerostin, the product of the SOST gene [40]. Mutations of SOST are found in patients with sclerosteosis, a syndrome of sclerosing skeletal dysplasia [60] (see Section 4). Because sclerostin was subsequently shown to be a new member of BMP antagonist expressed in bones and cartilages [40–42], USAG-1 is postulated to be a BMP antagonist expressed in the kidney [38].

3.3. USAG-1 is a BMP antagonist

USAG-1 is a 28–30 kDa secretory protein and behaved as a monomer [38,61], in spite that a number of BMP antagonists form disulfide-bridged dimers. This is consistent with the fact that USAG-1 does not have the extra cysteine residues present in noggin and DAN, which are necessary to make inter-molecular disulfide bridges [17]. Recombinant USAG-1 protein binds to BMP-2, -4, -6, and -7 with high affinity, leading to the inhibition of BMP-2, -4, -6 or -7-induced alkaline phosphatase activities (ALP) in C2C12 cells [38] and MC3T3-E1 cells [61] dose-dependently, while sclerostin only inhibits BMP-6 and BMP-7 activities [40].

Furthermore, the activity of USAG-1 as a BMP antagonist was confirmed in vivo using *Xenopus* embryos [38]. Injection of synthetic mRNA encoding BMP antagonists to the ventral portion of *Xenopus* embryos inhibits the

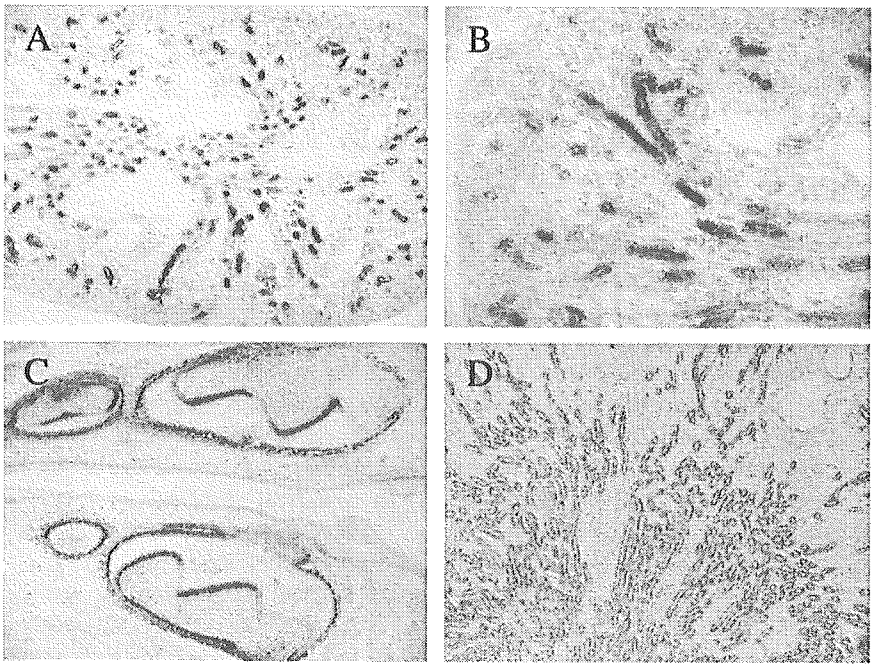

Fig. 2. Expression of USAG-1 mRNA: (A) ×40; (B) ×200. In E17.5 mouse embryos, the expression of USAG-1 is prominent in kidney tubules; and (C) in ameloblasts of teeth. In adult kidney, the expression of USAG-1 is confined to distal tubules in the kidney (D).

ventralizing signal of endogenous BMP, and induces secondary axis formation and hyperdorsalization of the embryos [62]. The injection of as little as 100 pg USAG-1 mRNA was sufficient to cause secondary axis formation, and injection of increasing doses of mRNA up to 1000 pg led to a corresponding increase in the frequency of secondary axis formation and hyperdorsalization, while embryos developed normally when irrelevant mRNA was injected. Furthermore, injection of USAG-1 mRNA into the animal pole of *Xenopus* embryos induced expression of NCAM in animal caps dose-dependently, but not that of muscle actin [38], indicating that USAG-1 directly antagonizes BMP signaling in *Xenopus* embryos.

3.4. Expression of USAG-1

In mouse embryogenesis, expression of USAG-1 mRNA was first detected on embryonic day 11.5 (E11.5) and increased towards E17.5 [38]. In situ hybridization of mouse embryos on E11.5 revealed the moderate expression of USAG-1 mRNA in branchial arches and pharynx. On E17.5, strong expression of USAG-1 mRNA was confined to kidney tubules and ameloblasts of teeth (Fig. 2A–C). In addition, moderate expression was observed in hair follicles, ganglia, choroids plexus and ependymal cells in the ventricles of the brain.

In adult tissues, the expression was by far most abundant in the kidney and is restricted to the epithelial cells of distal collecting tubules (Fig. 2D) [38]. No expression was observed in proximal tubules or blood vessels in the kidney. Thus, the cellular distribution of USAG-1 is overlapping with that of BMP-7 in the kidney [49]. Taken together with the fact that proximal tubule epithelial cells (PTECs) are the site of injuries in many types of kidney diseases, and that PTECs express the receptors for BMP-7 [49], we hypothesized the working model about the regulation of reno-protective action of BMP-7 (Fig. 3); in renal injuries, PTECs are mainly damaged and undertake EMT to fibloblast-like mesenchymal cells. BMP-7 secreted from distal tubules binds to the receptors in the PTECs, and inhibits EMT [59]. USAG-1 is also secreted from distal tubules, binds to BMP-7, and inhibits the reno-protective actions of BMP-7 by reducing the amount of "active BMP-7".

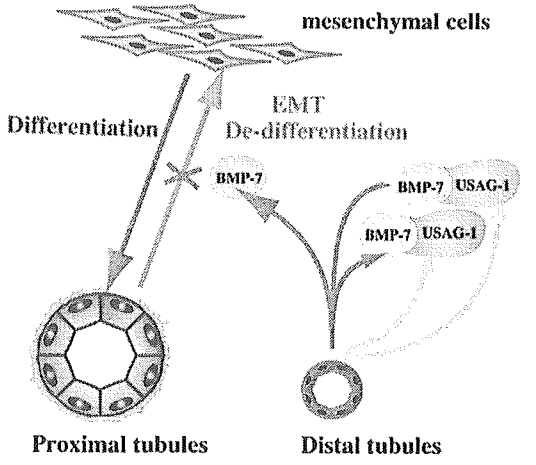

Fig. 3. Working model about the regulation of reno-protective action of BMP-7. In renal injuries, proximal tubule epithelial cells (PTECs) are mainly damaged and undertake EMT to fibloblast-like mesenchymal cells. BMP-7 secreted from distal tubules is reported to inhibit EMT of PTEC [104]. USAG-1 is also secreted from distal tubules, binds to BMP-7, and inhibits the reno-protective actions of BMP-7 by reducing the amount of active BMP-7.

Expression and possible functions of USAG-1 in developing teeth was further evaluated by Laurikkala et al. [61]. They independently identified ectodin (other name for USAG-1) as a BMP antagonist, and showed that ectodin/USAG-1 was intensely expressed in the peripheral part of the teeth, but was absent in and around the enamel knot signaling centers [61]. They also showed that ectodin/USAG-1 antagonized the BMP-mediated induction of *Msx2* expression in cultured tooth explants. Furthermore, BMP-2 and BMP-7 stimulated ectodin/USAG-1 expression in tooth explants, and the induction was prevented by SHH and FGF4, coexistent signals with BMPs in the enamel knot.

O'Shaunghnessy et al. reported the expression of Wise (other name for USAG-1; see Section 3.5) in the dermal papilla of hail follicle, and indicated that the expression pattern and level varied during the hair cycle [63]. It has been reported that noggin is expressed in hair follicles and plays a critical role in the induction of hair follicle by modulating the activities of BMPs [64,65]. Wise/USAG-1 might also share some roles with noggin in hair-follicle induction.

3.5. USAG-1 as a modulator of Wnt signaling

Recently, Itasaki et al. reported another function of USAG-1 as a context-dependent activator and inhibitor of Wnt signaling [66]. They carried out a screen to identify factors that can change the AP identity of neural tissue and found a Wise, *Xenopus* orthologue of USAG-1. Overexpression of Wise/USAG-1 in animal caps caused a posterior character, and the posteriorizing effect required Dishevelled [67] and β-catenin, which are components of the canonical Wnt signaling pathway, indicating that in this context Wise/USAG-1 activated the Wnt signaling cascade by mimicking some of the effects of Wnt ligands. In contrast, in an assay for secondary axis induction, Wise/USAG-1 antagonized the axis-inducing ability of Wnt8. They further demonstrated the physical interaction between Wise/USAG-1 and Wnt co-receptor, lipoprotein receptor-related protein 6 (LRP6) [68], and that Wise/USAG-1 is able to compete with Wnt8 for binding to LRP6.

Recently, close relationships between the Wnt and BMP pathways have been reported; for instance, the canonical Wnt antagonist DKK1 and noggin cooperate in head induction [69], while the expression of DKK1 is regulated by BMP-4 in limb development [70]. Furthermore, a BMP antagonist called Cerberus (see Section 5.2) has a binding site for Wnt proteins that is distinct from the BMP binding site, and antagonizes Wnt activities by directly binding to Wnt [71]. USAG-1 might also have dual activities, and play as a molecular link between Wnt and BMP signaling pathway.

4. Sclerostin

Sclerostin, encoded by the SOST gene, is another newly defined BMP antagonist, abundantly expressed in long bones and cartilages [40–42]. The SOST gene was originally identified as the gene responsible for a progressive sclerosing bone dysplasia known as sclerosteosis, an autosomal recessive disorder [60]. Sclerostin binds to BMP-6 and BMP-7 with high affinity and to BMP-2 and BMP-4 with low affinity, leading to the inhibition of BMP-6 and BMP-7 activities [40]. There has been a controversy about the cell type expressing sclerostin [40–42], however, van Bezooijen et al. recently elegantly showed that sclerostin is expressed exclusively by osteocytes, and inhibits the differentiation and mineralization of murine preosteoblastic cells [42]. Its unique localization and action on osteoblasts suggested that sclerostin might be the previously proposed osteocyte-derived factor that is transported to osteoblasts at the bone surface and inhibits bone formation [42].

In scleosteosis, loss of sclerostin might prolong the active bone-forming phase of osteoblasts, resulting in the increased bone mass. Winkler et al. reported that transgenic mice overexpressing SOST/sclerostin exhibited low bone mass and decreased bone strength as the result of a significant reduction in osteoblast activity and subsequently, bone formation [41]. Based on its suppressive role in bone formation, sclerostin could be a therapeutic target for the treatment of osteoporosis.

Although three groups independently reported that sclerostin is a novel BMP antagonist [40–42], there is a partial disagreement in its mechanism of action; while Kusu et al. and Winkler et al. reported that sclerostin is a classical BMP antagonist and inhibits BMP-induced Smad phosphorylation and ALP [40,41], van Bezooijen et al. reported that sclerostin does not inhibit short-term response to BMP such as Smad phosphorylation [42]. Further investigation would be needed to elucidate mechanism of action of sclerostin.

High bone mass diseases are also caused by gain-of-function mutations in LRP5 [72], a co-receptor for Wnt proteins, and the clinical features are quite similar to those of sclerosteosis. In addition, close interactions between BMP and Wnt signaling pathways are reported in osteoblastic cells [73,74]. Recently Winkler et al. reported that Wnt induces osteoblast differentiation through BMPs, and that BMP antagonists, such as sclerostin and noggin inhibit the Wnt-induced osteoblast differentiation [75]. The induction of BMP proteins in this autocrine loop is essential for Wnt-induced osteoblast differentiation.

Furthermore, high affinity binding between noggin and sclerostin was reported, and that noggin–sclerostin complex was competitive with BMP binding, and mutually attenuated the activity of each BMP antagonist [76]. These data demonstrate the possibility that function of noggin and sclerostin are pleiotrophic. They affect BMP signaling pathway negatively as BMP antagonists, but when their expression overlaps, they might form a complex, and BMP are available to bind to their receptors and induce downstream signaling pathways.

5. Other members of the DAN family

Differential screening-selected gene aberrative in neuroblastoma (DAN) family is composed of at least seven proteins: Dan, Cerberus, coco, PRDC, gremlin, sclerostin and USAG-1. All of them are conserved proteins with a signal peptide for secretion, putative N-linked glycosylation sites, and a cystine-knot motif in the carboxyl terminus [17]. Outside the cystine-knot motif, members of the DAN family have limited homology.

5.1. Dan

Dan gene (also called NO3) was first identified as a gene downregulated in *src*-transformed fibroblasts [36] and overexpression of DAN suppresses the tumorigenic activity of transformed fibroblasts [37,77,78]. Dan can bind BMP-2 and -4 at high concentrations; however, it is not clear whether the binding is physiologically relevant, because Dan also binds to GDF-5 more efficiently [79]. Dan mRNA is localized in many developing axon tracts, although Dan deficient mice have only subtle defects [79].

5.2. Cerberus/Cer1

Cerberus was identified in a search for transcripts that are abundantly expressed in Spemann organizer of *Xenopus* embryos [80], and injection of Cerberus mRNA into *Xenopus* embryos causes unique phenotype of inducing an ectopic head without trunk formation [71]. Trunk formation requires Nodal and Wnt signaling, whereas head induction requires inhibition of Wnt and BMP signaling. Cerberus, as a multifunctional antagonist, inhibits all three signaling pathways, which leads to simultaneous head formation and trunk inhibition [71]. Cerberus binds to BMP-4 and inhibits the activities, while it binds to Wnt and nodal by separate sites and inhibits these signaling pathways as well.

Although mouse protein Cerberus-like (mCer1) is distantly related to *Xenopus* Cerberus [81], it does not directly inhibit Wnt signals, and is unclear whether it is a true mouse orthologue. Homozygous null mutants for mCer1 show no anterior patterning defects, are born alive, and are fertile [82]. Since mCer1 and *Xenopus* Cerberus differ in biochemical activities, there might be additional Cerberus-like protein, which may compensate for the loss of mCer-1.

5.3. Coco

Recently, another closely related protein, named Coco was discovered in a screen for Smad7-induced genes [35]. Coco blocks BMP/TGFβ signaling in the ectoderm and regulates cell fate specification and competence prior to the onset of neural induction. In addition, Coco acts as a neural inducer and induces ectopic headlike structures in neurula staged embryos. This gene is expressed maternally in an animal to vegetal gradient, and its expression levels decline rapidly following gastrulation. Coco can inhibit Wnt signaling, and might be a candidate for the mouse orphologue for *Xenopus* Cerberus [35].

5.4. Protein related to DAN and Cerberus (PRDC)

PRDC was identified by gene trapping in embryonic stem cells [83]. PRDC binds to BMP-2 and BMP-4, and blocks the activities. PRDC transcripts are widely expressed showing higher levels in ovary, brain, and spleen. PRDC is expressed in granulosa cells of the ovaries, and might play some roles in follicular development by antagonizing the actions of BMPs.

5.5. Gremlin

Gremlin was identified from a *Xenopus* ovarian library for activities inducing secondary axis [22]. Gremlin is a 28-kDa protein, and binds to BMP-2/-4 and inhibits their binding to the receptors.

Gremlin-deficient mice are neonatally lethal because of the lack of kidneys and septation defects in lung [84]. In early limb buds, mesenchymal gremlin is required to establish a functional apical ectodermal ridge and the epithelial–mesenchymal feedback signaling that propagates the sonic hedgehog morphogen [85]. Furthermore, gremlin-mediated BMP antagonism is essential to induce metanephric kidney development [84].

Gremlin is also known as DRM (down-regulated by v-*mos*) because it was identified as a gene that down-regulated in *mos*-transformed cells [33,34]. Another name for gremlin is IHG-2 (induced in high glucose 2) because its expression in cultured kidney mesangial cells is induced by high ambient glucose, mechanical strain, and TGF-β [86]. The expression of gremlin in the kidney increased in streptozotocin-induced diabetic nephropathy [50]. Although both USAG-1 and gremlin are expressed in the kidney and seem to play some roles in kidney diseases, there are several differences: first, target molecules of gremlin are considered to be BMP-2 and BMP-4 [22], whereas USAG-1 antagonizes BMP-7 as well [38]; second, gremlin is expressed in mesangial cells in the kidney glomerulus [86], while the expression of USAG-1 is confined to the epithelial cells of distal tubules [38]. Thus these two BMP antagonists seem to play distinct roles in the development and progression of kidney diseases.

6. Noggin

Noggin is a 32 kDa glycoprotein secreted by Spemann organizer of *Xenopus* embryos [87], and is found to rescue dorsal development in the ultra-violet-induced ventralized embryos. Noggin antagonizes the action of BMPs, and induces neural tissue and dorsalizes ventral mesoderm [3,88]. Noggin binds to BMP-2 and BMP-4 with high

affinity and to BMP-7 with low affinity, and prevent BMPs from binding to its receptors. Recently, Groppe et al. reported the crystal structure of noggin–BMP-7 complex, and demonstrated that noggin inhibits BMP signaling by blocking the molecular interfaces of the binding epitopes for both type I and type II receptors [30].

In mice, noggin is expressed in the node, notochord, dorsal somite, condensing cartilage, and immature chondrocytes and is required for patterning of the neural tube and somites [89,90]. The function of noggin is essential in skeletal and joint development: homozygous mice for noggin-null mutant had excess cartilage and failed to initiate joint formation [89]. Although heterozygous mice for noggin-null mutant appear normal, heterozygous mutations in the human locus result in individuals with apical joint fusions, indicating functional haploinsufficiency [91,92]. Furthermore, transgenic mice overexpressing noggin in mature osteocalcin-positive osteoblasts showed dramatic decreases in bone mineral density and bone formation rates [93].

Craniosynostosis, or premature cranial suture fusion, results in an abnormal skull shape, blindness and mental retardation. Recent studies have demonstrated that gain-of-function mutations in fibroblast growth factor receptors (fgfr) are associated with syndromic forms of craniosynostosis [94,95]. Warren et al. reported that noggin is expressed postnatally in the suture mesenchyme of patent, but not fusing, cranial sutures, and that the expression of noggin is suppressed by FGF2 and syndromic fgfr signaling [31]. In addition, noggin misexpression prevents cranial suture fusion. They conclude that syndromic fgfr-mediated craniosynostoses may be the result of inappropriate down-regulation of noggin expression.

Beyond the skeletal development, noggin also plays essential roles in various tissues; noggin is expressed in the follicular mesenchyme, where it neutralizes the inhibitory action of BMP4 on hair-follicle induction [64,65]. Furthermore, noggin antagonizes BMP signaling to regulate the stem cell niche during neurogenesis [20].

7. Chordin

Chordin, another BMP antagonist found in Spemann organizer [96,97], is a 120-kDa large protein, which contains four cysteine-rich domains of about 70 amino acids each [96–98].

Chordin has a homolog in *Drosophila*, called short gastrulation (sog), which binds to decapentaplegic, a BMP2/4 homologue. Chordin binds to BMP-2 and BMP-4, and prevents their interaction with BMP receptors [96]. The activities of chordin are further regulated by a metalloprotease Tolloid [99], and twisted gastrulation (see Section 8).

Chordin deficient mice demonstrate, at low penetrance, early lethality and a ventralized gastrulation phenotype [100]. The mutant embryos that survive die perinatally, displaying an extensive array of malformations in pharyngeal and cardiovascular organization that encompass most features of DiGeorge and Velo-Cardio-Facial syndromes in humans [101].

Double knockout mice for noggin/chordin display severe defects in the development of head and facial structures, and demonstrate disrupted mesoderm development and abnormal left to right patterning [100].

8. Twisted gastrulation (Tsg)

Twisted gastrulation (Tsg) is a secreted protein that regulates BMP signaling in the extracellular space through its direct interaction with BMP and chordin [26–28], and the ternary complex of BMP/Chordin/Tsg is cleaved by the metalloprotease, Tolloid [99].

First, Tsg promotes the formation of stable ternary BMP/chordin/Tsg complexes. Because this ternary complex prevents binding of BMP to its receptors, in this aspect Tsg behaves as a BMP antagonist. Second, the stability of these inhibitory ternary complexes is controlled by the Tolloid metalloprotease, which cleaves chordin at specific sites. Because the presence of Tsg makes chordin susceptible for cleavage by Tolloid, Tsg promotes the degradation of chordin by Tolloid, and releases BMP that is now able to signal through its receptors. In this second aspect, Tsg functions to increase BMP activity.

Tsg-deficient mice were born healthy, but more than half of the neonatal pups showed severe growth retardation shortly after birth and displayed dwarfism with delayed endochondral ossification and lymphopenia, followed by death within a month [102]. Tsg-deficient thymus was atrophic, and phosphorylation of Smad1 was augmented in the thymocytes, suggesting enhanced BMP-4 signaling in the thymus. Since BMP-4 promotes skeletogenesis and inhibits thymus development [103], these findings suggest that Tsg acts as both a BMP-4 agonist in skeletogenesis and a BMP-4 antagonist in T-cell development.

9. Summary and future directions

Although the functions of BMPs are spaciotemporally regulated in embryonic and postnatal developmental processes, the expression of BMPs and the receptors is not strictly restricted to certain areas. Instead, the expression of BMP antagonists is precisely regulated, and edges the boundaries of BMP functions. In other words, BMP antagonists act as on/off switch of BMP functions. While developmental functions of BMPs have been extensively studied, the biological functions of BMPs after birth remain to be elucidated, probably due to the embryonic and perinatal lethality or developmental defect of BMP-deficient mice. Mice deficient of or overexpressing certain BMP antagonists can be powerful tools to elucidate the biological function of BMPs after birth.

Furthermore, USAG-1 and sclerostin are unique in their tissue-specific expression, biochemical behavior, and their possible functions after birth. Future investigation would provide valuable information on their pathophysiological functions and give a rationale for the therapeutic approach against these proteins.

Acknowledgements

I thank Drs. M. Yanagisawa, T. Sakurai, E. Nishi for helpful advices, and Dr. A.H. Reddi for giving me an opportunity to write this review.

Reference

[1] Massague J, Chen YG. Controlling TGF-β signaling. Genes Dev 2000;14(6):627–44.
[2] Canalis E, Economides AN, Gazzerro E. Bone morphogenetic proteins, their antagonists, and the skeleton. Endocr Rev 2003;24(2):218–35.
[3] Reddi AH. Interplay between bone morphogenetic proteins and cognate binding proteins in bone and cartilage development: noggin, chordin and DAN. Arthritis Res 2001;3(1):1–5.
[4] Attisano L, Wrana JL. Signal transduction by members of the transforming growth factor-β superfamily. Cytokine Growth Factor Rev 1996;7(4):327–39.
[5] Reddi AH. Bone morphogenetic proteins and skeletal development: the kidney–bone connection. Pediatr Nephrol 2000;14(7): 598–601.
[6] Urist MR. Bone: formation by autoinduction. Science 1965;150 (698):893–9.
[7] Wozney JM, Rosen V, Celeste AJ, Mitsock LM, Whitters MJ, Kriz RW, et al. Novel regulators of bone formation: molecular clones and activities. Science 1988;242(4885):1528–34.
[8] Hogan BL. Bone morphogenetic proteins in development. Curr Opin Genet Dev 1996;6(4):432–8.
[9] Wang EA. Bone morphogenetic proteins (BMPs): therapeutic potential in healing bony defects. Trends Biotechnol 1993;11(9):379–83.
[10] Klahr S. The bone morphogenetic proteins (BMPs). Their role in renal fibrosis and renal function. J Nephrol 2003;16(2):179–85.
[11] Hruska KA, Saab G, Chaudhary LR, Quinn CO, Lund RJ, Surendran K. Kidney–bone, bone–kidney, and cell–cell communications in renal osteodystrophy. Semin Nephrol 2004;24(1):25–38.
[12] Zeisberg M, Muller GA, Kalluri R. Are there endogenous molecules that protect kidneys from injury? The case for bone morphogenic protein-7 (BMP-7). Nephrol Dial Transplant 2004;19(4):759–61.
[13] Miyazono K, Kusanagi K, Inoue H. Divergence and convergence of TGF-β/BMP signaling. J Cell Physiol 2001;187(3):265–76.
[14] Morse JH, Deng Z, Knowles JA. Genetic aspects of pulmonary arterial hypertension. Ann Med 2001;33(9):596–603.
[15] Chang CF, Lin SZ, Chiang YH, Morales M, Chou J, Lein P, et al. Intravenous administration of bone morphogenetic protein-7 after ischemia improves motor function in stroke rats. Stroke 2003;34(2):558–64.
[16] Howe JR, Bair JL, Sayed MG, Anderson ME, Mitros FA, Petersen GM, et al. Germline mutations of the gene encoding bone morphogenetic protein receptor 1A in juvenile polyposis. Nat Genet 2001;28(2):184–7.
[17] Avsian-Kretchmer O, Hsueh AJ. Comparative genomic analysis of the eight-membered ring cystine-knot-containing bone morphogenetic protein antagonists. Mol Endocrinol 2004;18(1):1–12.
[18] Wagner DS, Mullins MC. Modulation of BMP activity in dorsal–ventral pattern formation by the chordin and ogon antagonists. Dev Biol 2002;245(1):109–23.
[19] Wessely O, Agius E, Oelgeschlager M, Pera EM, De Robertis EM. Neural induction in the absence of mesoderm: β-catenin-dependent expression of secreted BMP antagonists at the blastula stage in *Xenopus*. Dev Biol 2001;234(1):161–73.
[20] Lim DA, Tramontin AD, Trevejo JM, Herrera DG, Garcia-Verdugo JM, Alvarez-Buylla A. Noggin antagonizes BMP signaling to create a niche for adult neurogenesis. Neuron 2000;28(3):713–26.
[21] Vitt UA, Hsu SY, Hsueh AJ. Evolution and classification of cystine-knot-containing hormones and related extracellular signaling molecules. Mol Endocrinol 2001;15(5):681–94.
[22] Hsu DR, Economides AN, Wang X, Eimon PM, Harland RM. The *Xenopus* dorsalizing factor Gremlin identifies a novel family of secreted proteins that antagonize BMP activities. Mol Cell 1998;1(5):673–83.
[23] Pearce JJ, Penny G, Rossant J. A mouse Cerberus/Dan-related gene family. Dev Biol 1999;209(1):98–110.
[24] Topol LZ, Marx M, Laugier D, Bogdanova NN, Boubnov NV, Clausen PA, et al. Identification of *drm*, a novel gene whose expression is suppressed in transformed cells and which can inhibit growth of normal but not transformed cells in culture. Mol Cell Biol 1997;17(8):4801–10.
[25] Oelgeschlager M, Larrain J, Geissert D, De Robertis EM. The evolutionarily conserved BMP-binding protein twisted gastrulation promotes BMP signaling. Nature 2000;405(6788):757–63.
[26] Ross JJ, Shimmi O, Vilmos P, Petryk A, Kim H, Gaudenz K, et al. Twisted gastrulation is a conserved extracellular BMP antagonist. Nature 2001;410(6827):479–83.
[27] Scott IC, Blitz IL, Pappano WN, Maas SA, Cho KW, Greenspan DS. Homologues of Twisted gastrulation are extracellular cofactors in antagonism of BMP signaling. Nature 2001;410(6827): 475–8.
[28] Chang C, Holtzman DA, Chau S, Chickering T, Woolf EA, Holmgren LM, et al. Twisted gastrulation can function as a BMP antagonist. Nature 2001;410(6827):483–7.
[29] Dionne MS, Brunet LJ, Eimon PM, Harland RM. Noggin is required for correct guidance of dorsal root ganglion axons. Dev Biol 2002;251(2):283–93.
[30] Groppe J, Greenwald J, Wiater E, Rodriguez-Leon J, Economides AN, Kwiatkowski W, et al. Structural basis of BMP signaling inhibition by the cystine-knot protein Noggin. Nature 2002;420(6916):636–42.
[31] Warren SM, Brunet LJ, Harland RM, Economides AN, Longaker MT. The BMP antagonist noggin regulates cranial suture fusion. Nature 2003;422(6932):625–9.
[32] Minabe-Saegusa C, Saegusa H, Tsukahara M, Noguchi S. Sequence and expression of a novel mouse gene PRDC (protein related to DAN and Cerberus) identified by a gene trap approach. Dev Growth Differ 1998;40(3):343–53.
[33] Topol LZ, Modi WS, Koochekpour S, Blair DG. DRM/GREMLIN (CKTSF1B1) maps to human chromosome 15 and is highly expressed in adult and fetal brain. Cytogenet Cell Genet 2000;89(1–2):79–84.
[34] Topol LZ, Bardot B, Zhang Q, Resau J, Huillard E, Marx M, et al. Biosynthesis, post-translation modification, and functional characterization of Drm/Gremlin. J Biol Chem 2000;275(12):8785–93.
[35] Bell E, Munoz-Sanjuan I, Altmann CR, Vonica A, Brivanlou AH. Cell fate specification and competence by Coco, a maternal BMP TGF-β and Wnt inhibitor. Development 2003;130(7):1381–9.
[36] Ozaki T, Sakiyama S. Molecular cloning and characterization of a cDNA showing negative regulation in v-src-transformed 3Y1 rat fibroblasts. Proc Natl Acad Sci USA 1993;90(7):2593–7.
[37] Ozaki T, Sakiyama S. Tumor-suppressive activity of N03 gene product in v-src-transformed rat 3Y1 fibroblasts. Cancer Res 1994;54(3):646–8.

[38] Yanagita M, Oka M, Watabe T, Iguchi H, Niida A, Takahashi S, et al. USAG-1: a bone morphogenetic protein antagonist abundantly expressed in the kidney. Biochem Biophys Res Commun 2004;316(2):490–500.
[39] Simmons DG, Kennedy TG. Uterine sensitization-associated gene-1: a novel gene induced within the rat endometrium at the time of uterine receptivity/sensitization for the decidual cell reaction. Biol Reprod 2002;67(5):1638–45.
[40] Kusu N, Laurikkala J, Imanishi M, Usui H, Konishi M, Miyake A, et al. Sclerostin is a novel secreted osteoclast-derived bone morphogenetic protein antagonist with unique ligand specificity. J Biol Chem 2003;278(26):24113–7.
[41] Winkler DG, Sutherland MK, Geoghegan JC, Yu C, Hayes T, Skonier JE, et al. Osteocyte control of bone formation via sclerostin, a novel BMP antagonist. EMBO J 2003;22(23):6267–76.
[42] van Bezooijen RL, Roelen BA, Visser A, van der Wee-Pals L, de Wilt E, Karperien M, et al. Sclerostin is an osteocyte-expressed negative regulator of bone formation, but not a classical BMP antagonist. J Exp Med 2004;199(6):805–14.
[43] Helder MN, Ozkaynak E, Sampath KT, Luyten FP, Latin V, Oppermann H, et al. Expression pattern of osteogenic protein-1 (bone morphogenetic protein-7) in human and mouse development. J Histochem Cytochem 1995;43(10):1035–44.
[44] Vukicevic S, Stavljenic A, Pecina M. Discovery and clinical applications of bone morphogenetic proteins. Eur J Clin Chem Clin Biochem 1995;33(10):661–71.
[45] Vukicevic S, Kopp JB, Luyten FP, Sampath TK. Induction of nephrogenic mesenchyme by osteogenic protein 1 (bone morphogenetic protein 7). Proc Natl Acad Sci USA 1996;93(17):9021–6.
[46] Ozkaynak E, Schnegelsberg PN, Oppermann H. Murine osteogenic protein (OP-1): high levels of mRNA in kidney. Biochem Biophys Res Commun 1991;179(1):116–23.
[47] Luo G, Hofmann C, Bronckers AL, Sohocki M, Bradley A, Karsenty G. BMP-7 is an inducer of nephrogenesis, and is also required for eye development and skeletal patterning. Genes Dev 1995;9(22):2808–20.
[48] Dudley AT, Lyons KM, Robertson EJ. A requirement for bone morphogenetic protein-7 during development of the mammalian kidney and eye. Genes Dev 1995;9(22):2795–807.
[49] Gould SE, Day M, Jones SS, Dorai H. BMP-7 regulates chemokine, cytokine, and hemodynamic gene expression in proximal tubule cells. Kidney Int 2002;61(1):51–60.
[50] Wang SN, Lapage J, Hirschberg R. Loss of tubular bone morphogenetic protein-7 in diabetic nephropathy. J Am Soc Nephrol 2001;12(11):2392–9.
[51] Hruska KA. Treatment of chronic tubulointerstitial disease: a new concept. Kidney Int 2002;61(5):1911–22.
[52] Morrissey J, Hruska K, Guo G, Wang S, Chen Q, Klahr S. Bone morphogenetic protein-7 improves renal fibrosis and accelerates the return of renal function. J Am Soc Nephrol 2002;13(Suppl. 1):S14–21.
[53] Dube PH, Almanzar MM, Frazier KS, Jones WK, Charette MF, Paredes A. Osteogenic protein-1: gene expression and treatment in rat remnant kidney model. Toxicol Pathol 2004;32(4):384–92.
[54] Almanzar MM, Frazier KS, Dube PH, Piqueras AI, Jones WK, Charette MF, et al. Osteogenic protein-1 mRNA expression is selectively modulated after acute ischemic renal injury. J Am Soc Nephrol 1998;9(8):1456–63.
[55] Vukicevic S, Basic V, Rogic D, Basic N, Shih MS, Shepard A, et al. Osteogenic protein-1 (bone morphogenetic protein-7) reduces severity of injury after ischemic acute renal failure in rat. J Clin Invest 1998;102(1):202–14.
[56] Hruska KA, Guo G, Wozniak M, Martin D, Miller S, Liapis H, et al. Osteogenic protein-1 prevents renal fibrogenesis associated with ureteral obstruction. Am J Physiol Renal Physiol 2000;279(1):F130–43.
[57] Wang S, Chen Q, Simon TC, Strebeck F, Chaudhary L, Morrissey J, et al. Bone morphogenic protein-7 (BMP-7), a novel therapy for diabetic nephropathy. Kidney Int 2003;63(6):2037–49.
[58] Zeisberg M, Bottiglio C, Kumar N, Maeshima Y, Strutz F, Muller GA, et al. Bone morphogenic protein-7 inhibits progression of chronic renal fibrosis associated with two genetic mouse models. Am J Physiol Renal Physiol 2003;285(6):F1060–7.
[59] Zeisberg M, Hanai J, Sugimoto H, Mammoto T, Charytan D, Strutz F, et al. BMP-7 counteracts TGF-β1-induced epithelial-to-mesenchymal transition and reverses chronic renal injury. Nat Med 2003;9(7):964–8.
[60] Brunkow ME, Gardner JC, Van Ness J, Paeper BW, Kovacevich BR, Proll S, et al. Bone dysplasia sclerosteosis results from loss of the SOST gene product, a novel cystine-knot-containing protein. Am J Hum Genet 2001;68(3):577–89.
[61] Laurikkala J, Kassai Y, Pakkasjarvi L, Thesleff I, Itoh N. Identification of a secreted BMP antagonist, ectodin, integrating BMP, FGF, and SHH signals from the tooth enamel knot. Dev Biol 2003;264(1):91–105.
[62] Harland R, Gerhart J. Formation and function of Spemann's organizer. Annu Rev Cell Dev Biol 1997;13:611–67.
[63] O'Shaughnessy RF, Yeo W, Gautier J, Jahoda CA, Christiano AM. The WNT signaling modulator, Wise, is expressed in an interaction-dependent manner during hair-follicle cycling. J Invest Dermatol 2004;123(4):613–21.
[64] Botchkarev VA, Botchkareva NV, Nakamura M, Huber O, Funa K, Lauster R, et al. Noggin is required for induction of the hair follicle growth phase in postnatal skin. FASEB J 2001;15(12):2205–14.
[65] Botchkarev VA, Botchkareva NV, Roth W, Nakamura M, Chen LH, Herzog W, et al. Noggin is a mesenchymally derived stimulator of hair-follicle induction. Nat Cell Biol 1999;1(3):158–64.
[66] Itasaki N, Jones CM, Mercurio S, Rowe A, Domingos PM, Smith JC, et al. Wise, a context-dependent activator and inhibitor of Wnt signaling. Development 2003;130(18):4295–305.
[67] Sokol SY. Analysis of dishevelled signaling pathways during *Xenopus* development. Curr Biol 1996;6(11):1456–67.
[68] Tamai K, Semenov M, Kato Y, Spokony R, Liu C, Katsuyama Y, et al. LDL-receptor-related proteins in Wnt signal transduction. Nature 2000;407(6803):530–5.
[69] del Barco Barrantes I, Davidson G, Grone HJ, Westphal H, Niehrs C. Dkk1 and noggin cooperate in mammalian head induction. Genes Dev 2003;17(18):2239–44.
[70] Grotewold L, Ruther U. The Wnt antagonist Dickkopf-1 is regulated by Bmp signaling and c-Jun and modulates programmed cell death. EMBO J 2002;21(5):966–75.
[71] Piccolo S, Agius E, Leyns L, Bhattacharyya S, Grunz H, Bouwmeester T, et al. The head inducer Cerberus is a multifunctional antagonist of Nodal BMP and Wnt signals. Nature 1999;397(6721):707–10.
[72] Gong Y, Slee RB, Fukai N, Rawadi G, Roman-Roman S, Reginato AM, et al. LDL receptor-related protein 5 (LRP5) affects bone accrual and eye development. Cell 2001;107(4):513–23.
[73] Fischer L, Boland G, Tuan RS. Wnt-3A enhances bone morphogenetic protein-2-mediated chondrogenesis of murine C3H10T1/2 mesenchymal cells. J Biol Chem 2002;277(34):30870–8.
[74] Bain G, Muller T, Wang X, Papkoff J. Activated β-catenin induces osteoblast differentiation of C3H10T1/2 cells and participates in BMP2 mediated signal transduction. Biochem Biophys Res Commun 2003;301(1):84–91.
[75] Winkler DG, Kung Sutherland MS, Ojala E, Turcott E, Geoghegan JC, Shpektor D, et al. Sclerostin inhibition of Wnt-3a-induced C3H10T1/2 cell differentiation is Indirect and mediated by BMP proteins. J Biol Chem 2004.
[76] Winkler DG, Yu C, Geoghegan JC, Ojala EW, Skonier JE, Shpektor D, et al. Noggin and sclerostin bone morphogenetic protein antagonists form a mutually inhibitory complex. J Biol Chem 2004;279(35):36293–8.

[77] Stanley E, Biben C, Kotecha S, Fabri L, Tajbakhsh S, Wang CC, et al. DAN is a secreted glycoprotein related to *Xenopus* Cerberus. Mech Dev 1998;77(2):173–84.
[78] Enomoto H, Ozaki T, Takahashi E, Nomura N, Tabata S, Takahashi H, et al. Identification of human DAN gene, mapping to the putative neuroblastoma tumor suppressor locus. Oncogene 1994;9(10): 2785–91.
[79] Dionne MS, Skarnes WC, Harland RM. Mutation and analysis of Dan, the founding member of the Dan family of transforming growth factor β antagonists. Mol Cell Biol 2001;21(2):636–43.
[80] Bouwmeester T, Kim S, Sasai Y, Lu B, De Robertis EM. Cerberus is a head-inducing secreted factor expressed in the anterior endoderm of Spemann's organizer. Nature 1996;382(6592):595–601.
[81] Biben C, Stanley E, Fabri L, Kotecha S, Rhinn M, Drinkwater C, et al. Murine Cerberus homologue mCer-1: a candidate anterior patterning molecule. Dev Biol 1998;194(2):135–51.
[82] Belo JA, Bachiller D, Agius E, Kemp C, Borges AC, Marques S, et al. Cerberus-like is a secreted BMP and nodal antagonist not essential for mouse development. Genesis 2000;26(4):265–70.
[83] Sudo S, Avsian-Kretchmer O, Wang LS, Hsueh AJ. Protein related to DAN and Cerberus is a bone morphogenetic protein antagonist that participates in ovarian paracrine regulation. J Biol Chem 2004;279(22):23134–41.
[84] Michos O, Panman L, Vintersten K, Beier K, Zeller R, Zuniga A. Gremlin-mediated BMP antagonism induces the epithelial–mesenchymal feedback signaling controlling metanephric kidney and limb organogenesis. Development 2004;131(14):3401–10.
[85] Khokha MK, Hsu D, Brunet LJ, Dionne MS, Harland RM. Gremlin is the BMP antagonist required for maintenance of Shh and Fgf signals during limb patterning. Nat Genet 2003;34(3):303–7.
[86] McMahon R, Murphy M, Clarkson M, Taal M, Mackenzie HS, Godson C, et al. IHG-2, a mesangial cell gene induced by high glucose, is human gremlin. Regulation by extracellular glucose concentration, cyclic mechanical strain, and transforming growth factor-β1. J Biol Chem 2000;275(14):9901–4.
[87] Smith WC, Harland RM. Expression cloning of noggin, a new dorsalizing factor localized to the Spemann organizer in *Xenopus* embryos. Cell 1992;70(5):829–40.
[88] Lamb TM, Knecht AK, Smith WC, Stachel SE, Economides AN, Stahl N, et al. Neural induction by the secreted polypeptide noggin. Science 1993;262(5134):713–8.
[89] Brunet LJ, McMahon JA, McMahon AP, Harland RM. Noggin, cartilage morphogenesis, and joint formation in the mammalian skeleton. Science 1998;280(5368):1455–7.
[90] McMahon JA, Takada S, Zimmerman LB, Fan CM, Harland RM, McMahon AP. Noggin-mediated antagonism of BMP signaling is required for growth and patterning of the neural tube and somite. Genes Dev 1998;12(10):1438–52.
[91] Gong Y, Krakow D, Marcelino J, Wilkin D, Chitayat D, Babul-Hirji R, et al. Heterozygous mutations in the gene-encoding noggin affect human joint morphogenesis. Nat Genet 1999;21(3):302–4.
[92] Marcelino J, Sciortino CM, Romero MF, Ulatowski LM, Ballock RT, Economides AN, et al. Human disease-causing NOG missense mutations: effects on noggin secretion, dimer formation, and bone morphogenetic protein binding. Proc Natl Acad Sci USA 2001;98(20):11353–8.
[93] Wu XB, Li Y, Schneider A, Yu W, Rajendren G, Iqbal J, et al. Impaired osteoblastic differentiation, reduced bone formation, and severe osteoporosis in noggin-overexpressing mice. J Clin Invest 2003;112(6):924–34.
[94] Cohen Jr MM. Craniosynostoses: phenotypic/molecular correlations. Am J Med Genet 1995;56(3):334–9.
[95] Wilkie AO. Craniosynostosis: genes and mechanisms. Hum Mol Genet 1997;6(10):1647–56.
[96] Piccolo S, Sasai Y, Lu B, De Robertis EM. Dorsoventral patterning in *Xenopus*: inhibition of ventral signals by direct binding of chordin to BMP-4. Cell 1996;86(4):589–98.
[97] Sasai Y, Lu B, Piccolo S, De Robertis EM. Endoderm induction by the organizer-secreted factors chordin and noggin in *Xenopus* animal caps. EMBO J 1996;15(17):4547–55.
[98] Larrain J, Bachiller D, Lu B, Agius E, Piccolo S, De Robertis EM. BMP-binding modules in chordin: a model for signaling regulation in the extracellular space. Development 2000;127(4):821–30.
[99] Wardle FC, Welch JV, Dale L. Bone morphogenetic protein 1 regulates dorsal–ventral patterning in early *Xenopus* embryos by degrading chordin, a BMP4 antagonist. Mech Dev 1999;86(1–2):75–85.
[100] Bachiller D, Klingensmith J, Kemp C, Belo JA, Anderson RM, May SR, et al. The organizer factors chordin and noggin are required for mouse forebrain development. Nature 2000;403(6770):658–61.
[101] Bachiller D, Klingensmith J, Shneyder N, Tran U, Anderson R, Rossant J, et al. The role of chordin/Bmp signals in mammalian pharyngeal development and DiGeorge syndrome. Development 2003;130(15):3567–78.
[102] Nosaka T, Morita S, Kitamura H, Nakajima H, Shibata F, Morikawa Y, et al. Mammalian twisted gastrulation is essential for skeletolymphogenesis. Mol Cell Biol 2003;23(8):2969–80.
[103] Graf D, Nethisinghe S, Palmer DB, Fisher AG, Merkenschlager M. The developmentally regulated expression of twisted gastrulation reveals a role for bone morphogenetic proteins in the control of T cell development. J Exp Med 2002;196(2):163–71.
[104] Kalluri R, Neilson EG. Epithelial–mesenchymal transition and its implications for fibrosis. J Clin Invest 2003;112(12):1776–84.

Uterine sensitization-associated gene–1 (USAG-1), a novel BMP antagonist expressed in the kidney, accelerates tubular injury

Motoko Yanagita,[1] Tomohiko Okuda,[1] Shuichiro Endo,[2] Mari Tanaka,[2] Katsu Takahashi,[3] Fumihiro Sugiyama,[4] Satoshi Kunita,[4] Satoru Takahashi,[4] Atsushi Fukatsu,[5] Masashi Yanagisawa,[6,7] Toru Kita,[2] and Takeshi Sakurai[6,8]

[1]COE Formation for Genomic Analysis of Disease Model Animals with Multiple Genetic Alterations, [2]Department of Cardiovascular Medicine, and [3]Department of Oral and Maxillofacial Surgery, Graduate School of Medicine, Kyoto University, Kyoto, Japan. [4]Laboratory Animal Resource Center, Institute of Basic Medical Sciences, University of Tsukuba, Ibaraki, Japan. [5]Department of Artificial Kidneys, Graduate School of Medicine, Kyoto University, Kyoto, Japan. [6]Yanagisawa Orphan Receptor Project, Exploratory Research for Advanced Technology (ERATO), Japan Science and Technology Agency, Tokyo, Japan. [7]Howard Hughes Medical Institute and Department of Molecular Genetics, University of Texas Southwestern Medical Center, Dallas, Texas, USA. [8]Department of Pharmacology, Institute of Basic Medical Sciences, University of Tsukuba, Ibaraki, Japan.

Dialysis dependency is one of the leading causes of morbidity and mortality in the world, and once end-stage renal disease develops, it cannot be reversed by currently available therapy. Although administration of large doses of bone morphogenetic protein–7 (BMP-7) has been shown to repair established renal injury and improve renal function, the pathophysiological role of endogenous BMP-7 and regulatory mechanism of its activities remain elusive. Here we show that the product of *uterine sensitization-associated gene–1* (*USAG1*), a novel BMP antagonist abundantly expressed in the kidney, is the central negative regulator of BMP function in the kidney and that mice lacking USAG-1 (*USAG1*$^{-/-}$ mice) are resistant to renal injury. *USAG1*$^{-/-}$ mice exhibited prolonged survival and preserved renal function in acute and chronic renal injury models. Renal BMP signaling, assessed by phosphorylation of Smad proteins, was significantly enhanced in *USAG1*$^{-/-}$ mice with renal injury, indicating that the preservation of renal function is attributable to enhancement of endogenous BMP signaling. Furthermore, the administration of neutralizing antibody against BMP-7 abolished renoprotection in *USAG1*$^{-/-}$ mice, indicating that USAG-1 plays a critical role in the modulation of renoprotective action of BMP and that inhibition of USAG-1 is a promising means of development of novel treatment for renal diseases.

Introduction

Despite a significant increase in understanding of the pathophysiology of renal diseases, the incidence of end-stage renal disease (ESRD) is still increasing. Tubular damage and interstitial fibrosis are the final common pathway leading to ESRD (1, 2), irrespective of the nature of the initial renal injury, and the degree of tubular damage parallels the impairment of renal function (2). Once tubular damage is established, it cannot be reversed or repaired by currently available treatment, and renal function deteriorates to renal failure, which is often life threatening (3). If we can come up with an agent that can reverse established tubular damage, it would significantly reduce the need for dialysis. Bone morphogenetic protein–7 (BMP-7) is a promising candidate for such an agent, because it is reported to protect the kidney from renal injury (4–8). BMP-7 is known to play essential roles in kidney development, because BMP-7–null mice die shortly after birth due to severe renal hypoplasia (9, 10). BMP-7 is also abundant in the adult kidney, especially in distal tubule epithelial cells (11, 12). Recently, several reports indicated that the expression of BMP-7 is decreased in renal disease models (5, 6, 13–16) and that administration of recombinant BMP-7 at pharmacological doses repairs chronic renal injury (4–8). However, the pathophysiological role and regulatory mechanism of endogenous BMP-7 remain elusive.

The local activity of endogenous BMP is controlled not only by regulation of its expression, but also by certain classes of molecules termed BMP antagonists (17). BMP antagonists function through direct association with BMP, thus inhibiting the binding of BMP to its receptors. *Uterine sensitization-associated gene–1* (*USAG1*) encodes a secreted protein and was initially found as a gene of unknown function whose expression was upregulated in sensitized endometrium of the rat uterus (18). Recently, Avsian-Kretchmer et al. suggested USAG-1 as a candidate for a novel BMP antagonist using bioinformatic analysis (19). Furthermore, Laurikkala et al. demonstrated USAG-1 to be a BMP antagonist expressed in teeth (20).

We independently identified USAG-1 to be a novel BMP antagonist, abundantly expressed in the kidney (21). The expression of USAG-1 is abundant in renal tubules and teeth in late embryogenesis and in adult tissues it is by far most abundant in the kidney, especially in the distal tubule with a pattern similar to that of BMP-7. From these findings, we hypothesized that USAG-1 might regulate the renoprotective action of BMP-7 in the adult kidney.

To evaluate this hypothesis, we generated *USAG1*-knockout (*USAG1*$^{-/-}$) mice and induced acute and chronic renal disease models in which renal tubules, but not glomeruli, were mainly damaged.

Nonstandard abbreviations used: BMP-7, bone morphogenetic protein–7; EMT, epithelial-mesenchymal transition; MCP-1, monocyte chemotactic protein-1; PTEC, proximal tubule epithelial cell; USAG1, uterine sensitization-associated gene–1; UUO, unilateral ureteral obstruction.

Conflict of interest: The authors have declared that no conflict of interest exists.

Citation for this article: *J. Clin. Invest.* **116**:70–79 (2006). doi:10.1172/JCI25445.

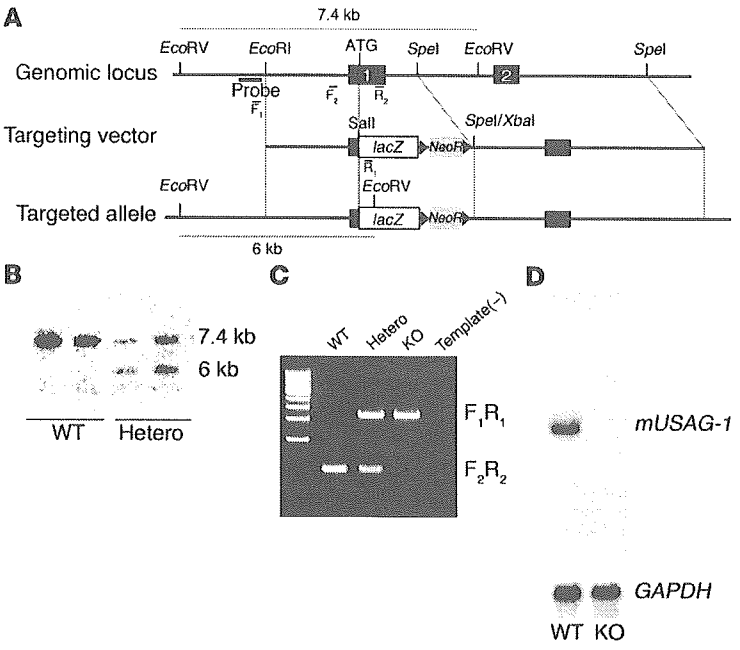

Figure 1
Generation of *USAG1*$^{-/-}$ mutation by gene targeting. (**A**) *USAG1*–null allele was generated by homologous recombination in ES cells. Exon 1 (black box) and part of the intron were replaced with a *lacZ* gene (white box) and the *Neo*R cassette (gray box). (**B**) Analysis of *USAG1*$^{+/+}$ (WT) and correctly targeted heterozygous (Hetero) ES cell clones by Southern blot analysis using 5′ genomic probe (thick black line in **A**). (**C**) PCR genotyping of F_2 littermates. Template(–) is the negative control. (**D**) Northern blot analysis of *USAG1* mRNA in the kidney of *USAG1*$^{+/+}$ and *USAG1*$^{-/-}$ (KO) mice.

Results

Generation and analysis of USAG1$^{-/-}$ *mice.* *USAG1*$^{-/-}$ mice were generated by deleting the first exon including the transcription initiation codon, the signal peptide, and the following 46 amino acids (Figure 1). *USAG1*$^{-/-}$ mice were born at the ratio expected according to Mendel's law of heredity and were viable, fertile, and appeared healthy except that they exhibited supernumerary teeth, both in the incisors and molars, and fused teeth in the molar region (Supplemental Figure 1; supplemental material available online with this article; doi:10.1172/JCI25445DS1). Although there was variation in the sites of extra teeth and fused teeth, this tooth phenotype was fully penetrant. Food consumption was not disturbed by this tooth phenotype in *USAG1*$^{-/-}$ mice (data not shown).

Attenuated acute tubular injury in USAG1$^{-/-}$ *mice.* To induce acute tubular injury, we utilized a cisplatin nephrotoxicity model (22–24). Administration of a nephrotoxic agent, cisplatin, to wild-type littermates caused acute tubular injury that resulted in severe renal failure. Within the first 3 days, 54% of wild-type mice died, while 92% of *USAG1*$^{-/-}$ mice survived the period (Figure 2A). The renal function of *USAG1*$^{-/-}$ mice on day 3 was significantly preserved compared with that in wild-type littermates (Figure 2B). Histological examination of the kidneys of wild-type mice on day 3 showed severe proximal tubular damage, while this change was markedly reduced in *USAG1*$^{-/-}$ mice (Figure 2, C and D). Expression of E-cadherin, a marker for tubular epithelial integrity (25), was markedly reduced in the kidneys of wild-type mice, while its expression was preserved in *USAG1*$^{-/-}$ mice (Figure 2E). Tubular apoptosis, a characteristic feature of tubular injury in cisplatin nephrotoxicity (23), was also significantly reduced in *USAG1*$^{-/-}$ mice (Figure 2F). As reported previously (24), cisplatin administration resulted in upregulation of TNF-α, IL-1β, monocyte chemotactic protein-1 (MCP-1), TGF-β1, and type IV collagen expression in the kidney of wild-type mice. However, the induction of these genes was completely abolished in *USAG1*$^{-/-}$ mice (Figure 2G). Infiltration of macrophages and monocytes in the kidney was also significantly reduced in *USAG1*$^{-/-}$ mice (Figure 2H), in accordance with the reduction of MCP-1 expression (Figure 2G). Expression of BMP-7 was comparable between wild-type mice and *USAG1*$^{-/-}$ mice before and after injection of cisplatin (Figure 2G).

Renal fibrosis is reduced in USAG1$^{-/-}$ *mice.* As a model of chronic renal injury, we performed unilateral ureteral obstruction (UUO) (26, 27) in both *USAG1*$^{-/-}$ mice and wild-type mice, and the kidneys were harvested 14 days after the operation. In wild-type mice, the obstructed kidney showed dilatation/degeneration of renal tubules and interstitial fibrosis, whereas the normal architecture was preserved in *USAG1*$^{-/-}$ mice, except for mild dilatation of tubules (Figure 3, A and B). Expression of E-cadherin was markedly reduced in the kidneys of wild-type mice, while its expression was preserved in *USAG1*$^{-/-}$ mice (Figure 3C). Furthermore, expression of α-SMA, a marker of tubulointerstitial myofibroblasts (28), was upregulated in the interstitium of the obstructed kidney of wild-type mice, while high expression of α-SMA was restricted to vascular smooth muscle cells in *USAG1*$^{-/-}$ mice (Figure 3D). Since expansion and fibrosis of the renal interstitium is another characteristic feature of UUO (6), we examined the deposition of type IV collagen, which is a normal component of the tubular basement membrane. The basement membranes of neighboring tubules are adjacent to each other in the normal kidney. In the obstructed kidney of wild-type mice, expansion of the interstitial component increased the distance between adjacent basement membranes, and type IV collagen produced by interstitial myofibroblasts was aberrantly expressed in the interstitium. However, in the obstructed kidney of *USAG1*$^{-/-}$ mice, the distance between the basement membranes was significantly smaller than that in wild-type mice (Figure 3E). Expression of TNF-α, IL-1β, MCP-1, TGF-β1, and type IV collagen was markedly upregulated on day 14 in the obstructed kidney of wild-type mice. In contrast, the induction of these genes was significantly attenuated, by 33%, 46%, 37%, 75%, and 23%, respectively, in *USAG1*$^{-/-}$ mice (Figure 3F). Expression of BMP-7 in the obstructed kidney was comparable in wild-type mice and *USAG1*$^{-/-}$ mice.

BMP signaling is enhanced in USAG1$^{-/-}$ *mice.* To evaluate whether the reduction in renal injury in *USAG1*$^{-/-}$ mice is attributable to enhanced BMP signaling, phosphorylation of Smad1/5/8 in the kidney was examined in both models (Figure 4). After the induction of kidney disease models, phosphorylation of Smad1/5/8 was hardly detected in wild-type mice, while in *USAG1*$^{-/-}$ mice, the phosphorylation was preserved in the nuclei of tubular epithelial cells (Figure 4A). To examine the specificity of the antibody against phospho-Smad1/5/8, we performed double immunostaining using anti-phospho-Smad1/5/8 antibody and anti–phospho-Smad2/3, and found that most of the nuclei positive for phospho-Smad1/5/8 were negative for phospho-Smad2/3 (Figure 4B), indicating the

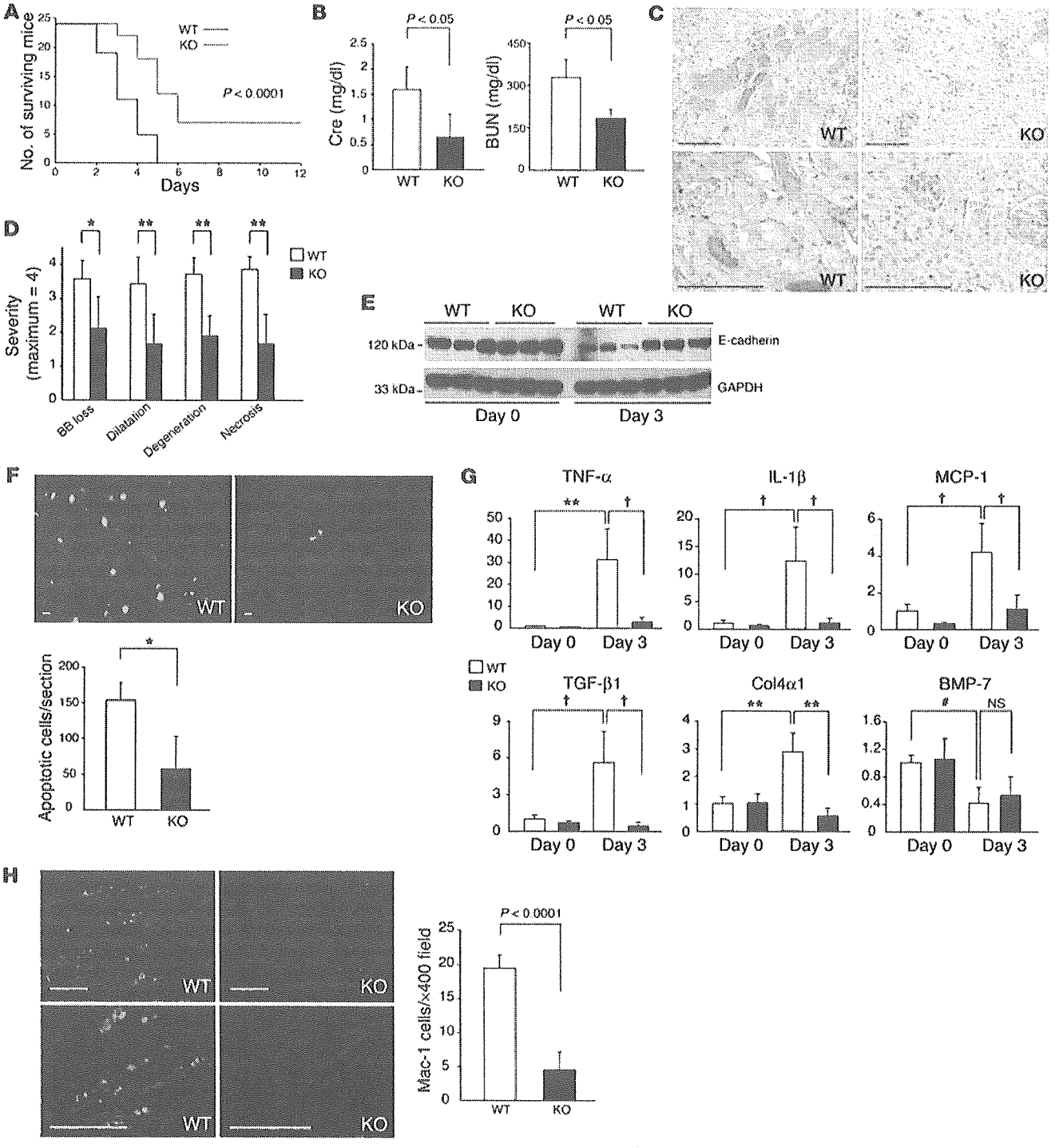

Figure 2

USAG1$^{-/-}$ mice showed less renal injury in cisplatin nephrotoxicity. (**A**) Survival curves of wild-type mice (black line) and *USAG1*$^{-/-}$ mice (red line) after cisplatin administration ($n = 24$). (**B**) Serum creatinine (Cre) and blood urea nitrogen (BUN) levels at 3 days after injection of cisplatin ($n = 6$). (**C**) Representative renal histological findings in wild-type mice and *USAG1*$^{-/-}$ mice on day 3. Scale bars: 100 μm. (**D**) Semiquantitative evaluation of morphologic kidney damage, expressed as relative severity on a scale from 0 to 4 ($n = 6$). Morphological findings were scored according to proximal tubule brush border loss (BB loss), tubule dilatation (Dilatation), tubule degeneration (Degeneration), and tubule necrosis (Necrosis). $^{*}P < 0.01$; $^{**}P < 0.001$. (**E**) E-cadherin expression in cisplatin nephrotoxicity. Kidney lysates were subjected to immunoblotting with anti–E-cadherin antibody. Representative data from 4 independent experiments are shown. (**F**) TUNEL staining of kidneys on day 3 of cisplatin nephrotoxicity. The number of TUNEL-positive cells per section was counted in transverse sections ($n = 6$). Scale bars: 10 μm. (**G**) Gene expression in cisplatin nephrotoxicity. Gene expression was determined by real-time RT-PCR. In each experiment, expression levels were normalized to the expression of GAPDH and expressed relative to mice on day 0. $n = 4$–6 for each experiment. $^{\dagger}P < 0.005$; $^{\#}P < 0.02$. Col4α1, collagen type IV α 1. (**H**) Infiltration of Mac-1–positive cells after cisplatin injection. The number of Mac-1–positive cells per field was counted in 10 consecutive fields ($n = 6$). Scale bars: 100 μm.

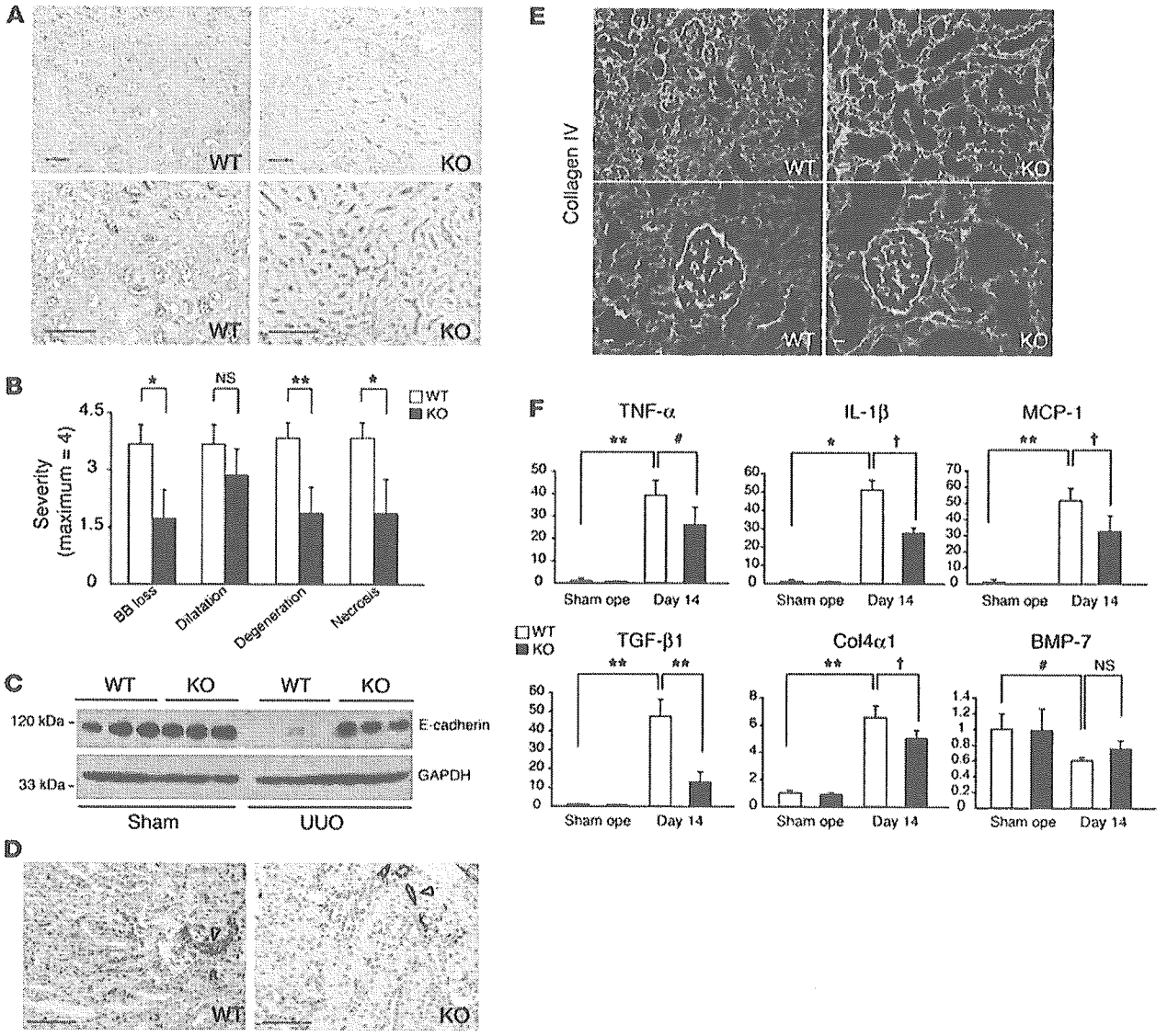

Figure 3

USAG1$^{-/-}$ mice showed reduced EMT and tubulointerstitial fibrosis in UUO. (**A**) Representative histology of the obstructed kidney in wild-type mice and *USAG1*$^{-/-}$ mice 14 days after the operation. Scale bars: 100 μm. (**B**) Semiquantitative evaluation of morphologic kidney damage in wild-type mice and *USAG1*$^{-/-}$ mice, expressed as relative severity on a scale from 0 to 4 ($n = 6$). (**C**) E-cadherin expression in UUO. Kidney lysates were subjected to immunoblotting with anti–E-cadherin antibody. Representative data from 4 independent experiments are shown. (**D**) Immunostaining of α-SMA in UUO. Arrowheads indicate vascular smooth muscle cells. (**E**) Immunostaining of type IV collagen in UUO. Scale bars: 10 μm. (**F**) Gene expression in UUO. Gene expression was determined by real-time RT-PCR. In each experiment, the expression levels were normalized to the expression of GAPDH and expressed relative to expression in mice on day 0. $n = 4$–6 for each experiment. $^{\#}P < 0.01$; $^{\dagger}P < 0.005$; $^{*}P < 0.001$; $^{**}P < 0.0001$. Sham ope, mice 14 days after sham operation; day 14, mice 14 days after UUO.

specificity of the antibody against phospho-Smad1/5/8. We also examined the phosphorylation of Smad1/5/8 in immunoblotting of kidney lysates and demonstrated that the phosphorylation was preserved in the kidneys of *USAG1*$^{-/-}$ mice, while it was downregulated in WT mice (Figure 4C). No difference was observed in the phosphorylation of Smad1/5/8 prior to disease induction between *USAG1*$^{-/-}$ mice and WT mice (Figure 4, A and C).

Blocking BMP-7 activity abolishes renoprotection in USAG1$^{-/-}$*mice.* To analyze the mechanism of renoprotection in *USAG1*$^{-/-}$mice, we administered a neutralizing antibody against BMP-7 to *USAG1*$^{-/-}$ mice in both kidney disease models. First we evaluated the specificity of the neutralizing activity of the antibody using an assay measuring alkaline phosphatase activity and phosphorylation of Smad1/5/8 in C2C12 cells induced by BMPs. Addition of the antibody inhibited the alkaline phosphatase activity and phosphorylation of Smad1/5/8 induced by BMP-7, but not by BMP-4 (Figure 5A) or BMP-2 (data not shown), indicating the specificity of the antibody. As a negative control, we used isotype-matched IgG2B. Next we administered a neutralizing antibody against BMP-7 to *USAG1*$^{-/-}$ mice with cisplatin nephrotoxicity. Of 7 mice treated with neutralizing antibody, 2 mice died on day 2 and 1 mouse died on day 3, while none of the mice treated with isotype-matched IgG2B

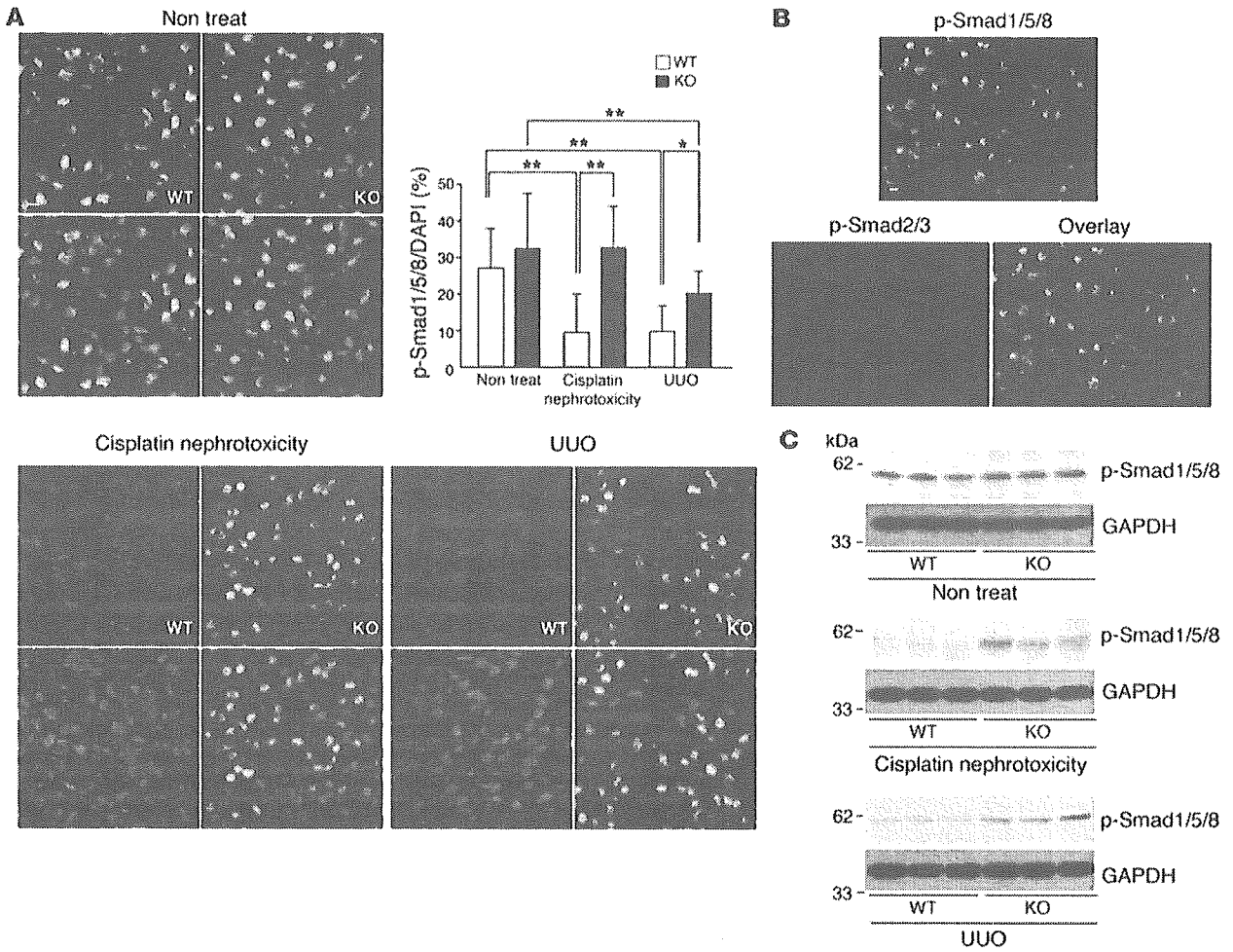

Figure 4

Enhanced BMP signaling in kidneys of *USAG1*$^{-/-}$ mice. (**A**) Phosphorylation of Smad1/5/8 in kidneys of *USAG1*$^{-/-}$ mice and WT mice. The number of pSmad1/5/8-positive nuclei (upper panels) was counted in 10 consecutive fields in each specimen and normalized by the number of DAPI-positive nuclei (lower panels). $n = 6$. Scale bar: 10 μm. $^{*}P < 0.001$; $^{**}P < 0.0001$. Non treat, mice without disease models. (**B**) Double immunostaining of phospho-Smad1/5/8 and phospho-Smad2/3. Almost all the nuclei positive for pSmad1/5/8 were negative for pSmad2/3. Scale bar: 10 μm. (**C**) Immunoblotting of phospho-Smad1/5/8 in kidney lysates prior to disease induction and in both kidney disease models. Representative data from 5 independent experiments are shown.

died within the first 3 days. Administration of neutralizing antibody also resulted in a deterioration of renal function measured by elevation of serum creatinine to a level similar to that in WT mice, while administration of IgG2B did not (Figure 5B). Furthermore, histological examination of the kidneys of *USAG1*$^{-/-}$ mice treated with neutralizing antibody demonstrated severely damaged proximal tubular epithelial cells, while these changes were absent in mice treated with IgG2B (Figure 5B). We also administered the neutralizing antibody to *USAG1*$^{-/-}$ mice with UUO and found that type IV collagen expression in the obstructed kidney was increased in *USAG1*$^{-/-}$ mice treated with neutralizing antibody, but not in those administered IgG2B (Figure 5C). Histological examination of the obstructed kidneys of *USAG1*$^{-/-}$ mice treated with neutralizing antibody demonstrated severe interstitial fibrosis, while this change was almost absent in mice treated with IgG2B (Figure 5C).

USAG1 is the most abundant BMP antagonist in adult kidney. Finally we analyzed the expression of USAG-1 and other BMP antagonists in adult kidneys using modified real-time PCR and in situ hybridization (Figure 6). To compare the expression levels of different genes in real-time PCR, we set the standard curve with the plasmid encoding each BMP antagonist at various concentrations and analyzed the copy number of each gene contained in kidney cDNA. Among known BMP antagonists, USAG-1 was by far the most abundant in the kidneys, and twisted gastrulation was the second most abundant BMP antagonist. We also analyzed the localization of BMP antagonists in the kidneys using in situ hybridization and found that the expression of USAG-1 was confined to distal tubules, as previously described (21), with a pattern similar to that of BMP-7 (12). Expression of twisted gastrulation was also detected in some distal tubules; however, the intensity of the signal was much lower than that of USAG-1, in accordance with the results of real-time PCR. Differential screening-selected gene aberrative in neuroblastoma (DAN) and protein related to DAN and Cerberus (PDRC) were faintly observed in the inner medulla, and other BMP antagonists were not detected with this method.

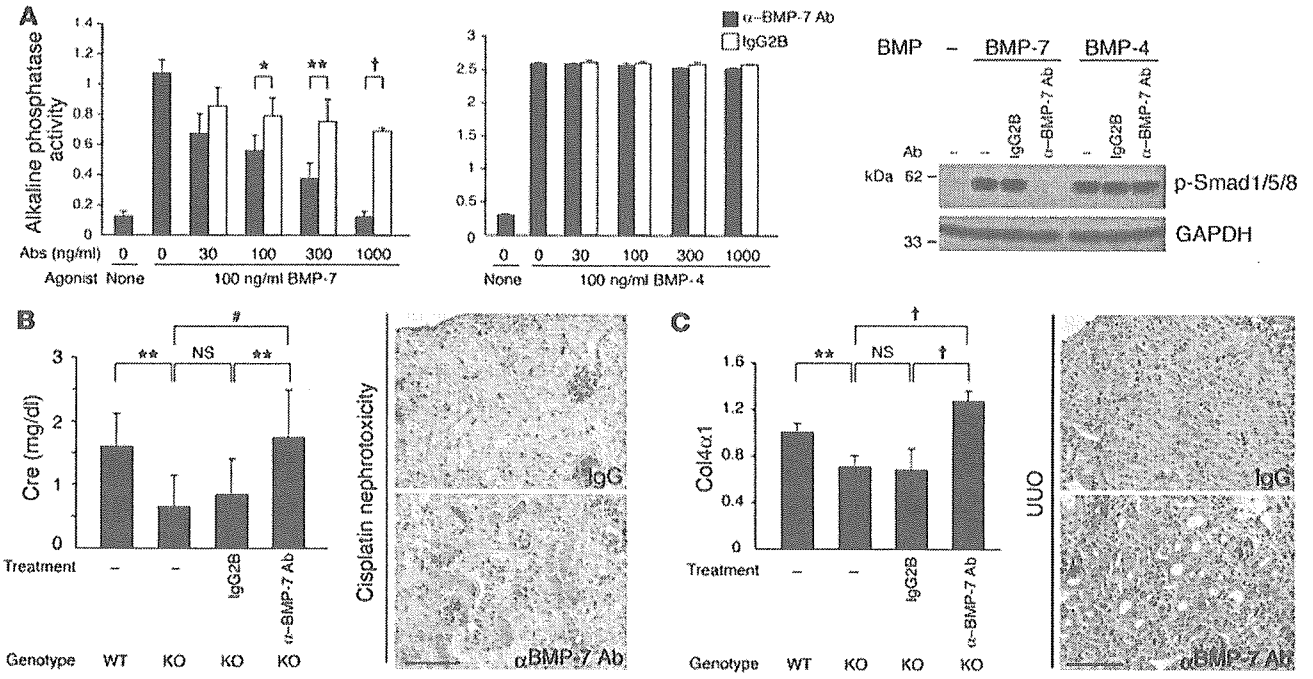

Figure 5

Blocking BMP-7 activity abolishes renoprotection in *USAG1*$^{-/-}$ mice. (**A**) Evaluation of neutralizing activity of anti–BMP-7 antibody. Anti–BMP-7 antibody inhibits alkaline phosphatase activity and phosphorylation of Smad1/5/8 induced by BMP-7, but not by BMP-4. (**B**) Serum creatinine level of *USAG1*$^{-/-}$ mice treated with anti–BMP-7 antibody and representative histological findings on day 3 of cisplatin nephrotoxicity. Scale bar: 100 μm. (**C**) Gene expression of type IV collagen in kidneys of *USAG1*$^{-/-}$ mice treated with anti–BMP-7 antibody and representative histological findings on day 14 of UUO. $^{*}P < 0.1$; $^{**}P < 0.01$; $^{\#}P < 0.001$; $^{\dagger}P < 0.0001$.

Discussion

Epithelial-mesenchymal transition (EMT) is a necessary step for renal fibrosis, as well as in embryonic development and tumor progression (29–31). TGF-β is known to stimulate EMT, while BMP-7 inhibits and reverses the transition (3). Zeisberg et al. recently reported that BMP-7 reverses TGF-β1–induced EMT and induces mesenchymal-epithelial transition in vitro (4, 32). They further demonstrated that administration of a pharmacological dose of BMP-7 resulted in regression of established lesions in the kidney and improved renal function. In this report, we demonstrated that deficiency of USAG-1, a novel BMP antagonist in the kidney, results in marked preservation of renal function by reinforcement of BMP signaling.

Based on these findings, we set the working hypothesis: in many types of renal disease, proximal tubule epithelial cells (PTECs) are the main site of injury (33) and undergo EMT, which causes loss of structural integrity of epithelial cells characterized by a reduction of E-cadherin expression and the induction of α-SMA in interstitial myofibroblasts (Figure 7A). BMP-7 secreted from distal tubules (12) inhibits EMT of PTECs and induces redifferentiation of mesenchymal cells to epithelial cells. USAG-1 produced from distal tubules binds to BMP-7 and inhibits its renoprotective action by interfering with binding to its receptors.

In addition to the inhibition of EMT, many other pharmacological actions of BMP-7 have been reported. Administration of recombinant BMP-7 inhibits the induction of inflammatory cytokine expression in the kidney (12), attenuates inflammatory cell infiltration (6), and reduces apoptosis of tubular epithelial cells in renal disease models (34) (Figure 7A). These phenomena are also observed in *USAG1*$^{-/-}$ mice, and the similarity between BMP-7–treated animals and *USAG1*$^{-/-}$ mice strongly supports our working model that deficiency of USAG-1 reinforces the renoprotective activities of BMP.

In accordance with this hypothesis, the renoprotection in *USAG1*$^{-/-}$ mice was abolished in both renal disease models when a neutralizing antibody against BMP-7 was administered (Figure 5). These results strongly support the hypothesis, and BMP-7 is a potent candidate for the counterpart of USAG-1.

We also observed preserved phosphorylation of Smad1/5/8 in the kidneys of *USAG1*$^{-/-}$ mice in both renal disease models, suggesting that BMP signaling was enhanced in *USAG1*$^{-/-}$ mice, while no difference was observed between WT and KO mice in phosphorylation of Smad1/5/8 prior to disease induction (Figure 4, A and C). We assume that BMP signaling prior to disease induction might be potent enough to cause full phosphorylation of Smad1/5/8 regardless of the presence or absence of USAG-1, while in the later stages of kidney diseases, BMP signaling is decreased and the presence of USAG-1 might cause a further reduction in BMP signaling.

Furthermore, we demonstrated that USAG-1 is by far the most abundant BMP antagonist in the kidney (Figure 6A). Because other BMP antagonists also antagonize BMP-7 activities (Supplemental Figure 2), we conclude that USAG-1 plays an important role in the modulation of BMP activities in the kidney not because of its ligand specificity, but because of its high expression among other BMP antagonists. In addition, the tissue localization of USAG-1 (Figure 6B) is quite similar to that of BMP-7 (12), and USAG-1 can effectively access and inactivate BMP-7 at the site of production.

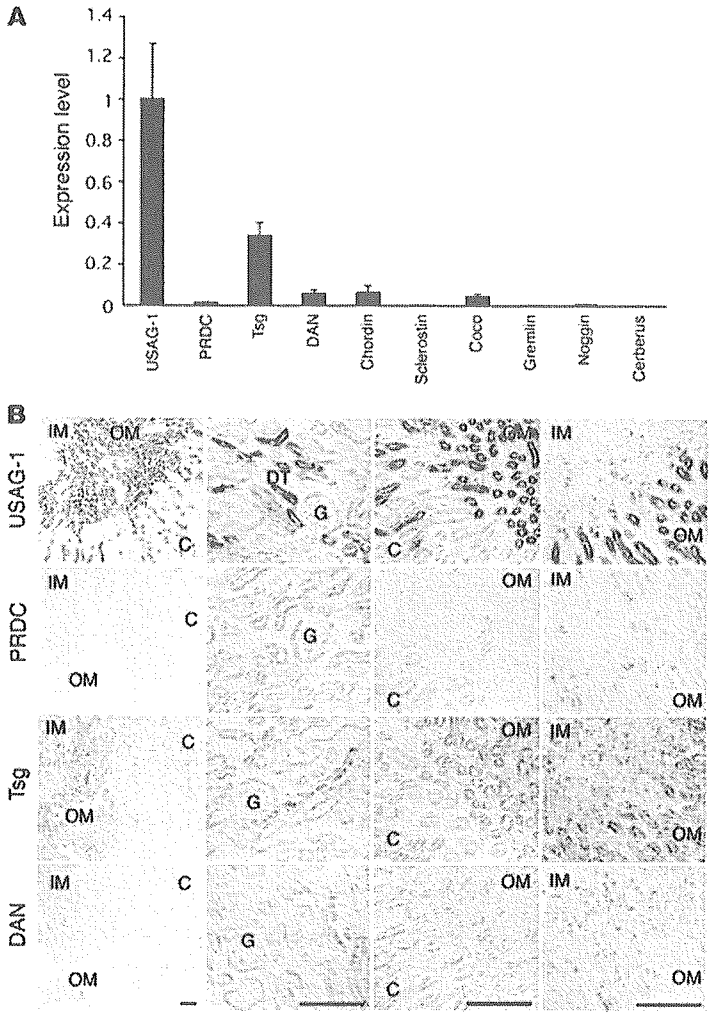

Figure 6

Expression of BMP antagonists in kidney. (**A**) Kidney cDNA of wild-type mice with Svj background was subjected to real-time PCR with various primers for BMP antagonists, and the standard curve was set using the plasmid encoding each BMP antagonist from concentrations of 1 pg/μl to 1 fg/μl. The values of each BMP antagonist in the kidney cDNA were multiplied by the length of the vectors and normalized to the value of USAG-1 expression (n = 4–5). Expression of USAG-1 was by far the most abundant in the kidney among other BMP antagonists. Tsg, twisted gastrulation. (**B**) Kidney sections were subjected to in situ hybridization with probes for all BMP antagonists. Expression of USAG-1 was confined to the distal tubular epithelial cells. Twisted gastrulation was also sparsely expressed in some distal tubules. Differential screening–selected gene aberrative in neuroblastoma (DAN) and protein related to DAN and Cerberus (PDRC) were faintly detected in the inner medulla. Expression of other BMP antagonists was not detected by this method. Scale bars: 100 μm. IM, inner medulla; OM, outer medulla; C, cortex; DT, distal tubule; G, glomerulus.

Although we illustrated USAG-1/BMP-7 binding as occurring outside of PTECs in Figure 7A, it might be possible that the binding occurs intracellularly within the secretory pathway in PTECs and that USAG-1 and BMP-7 are secreted in complex form. Further investigations are necessary to clarify this point.

Interestingly, the expression of USAG-1 decreased during the course of disease models (Supplemental Figure 3 and unpublished observations). We assume that the reduction of USAG-1 in renal diseases is a self-defense mechanism to minimize its inhibitory effect on BMP signaling. Because the reduction in USAG-1 expression in WT mice is not enough to overcome the reduction in BMP-7 expression, further reduction or abolishment of the action of USAG-1 is desirable for the preservation of renal function, and the results of the present study justify therapy targeted toward USAG-1. For example, drugs or neutralizing antibodies that inhibit binding between USAG-1 and BMP or gene-silencing therapy for *USAG1* would enhance the activity of endogenous BMP and might be a promising way to develop novel therapeutic methods for severe renal disease (Figure 7B). Because the expression of USAG-1 is confined to the kidney in adult mice and humans (21), it would be a better target for kidney-specific therapeutic trials. On the other hand, administration of recombinant BMP-7, whose target cells are widely distributed throughout the body, might produce some additional extrarenal actions, including beneficial effects, such as actions on renal osteodystrophy (35–39) and vascular calcification (40, 41).

Furthermore, these therapies targeted toward USAG-1 might protect the kidney during administration of nephrotoxic agents such as cisplatin. The pathological roles of USAG-1 in glomerular injury should be further elucidated before we undertake therapeutic trials against USAG-1.

Despite the essential role of BMP-7 in renal development, we did not observe any developmental abnormality in the kidney of *USAG1*$^{-/-}$ mice with this genetic background. We assume that there are many reasons for the lack of developmental abnormality: First, USAG-1 expression in the developing kidney is not apparent on embryonic day 11.5 (21), whereas BMP-7 expression is intense in the metanephric mesenchyme (42) with a pattern similar to that of gremlin (43). In the later stages, USAG-1 expression appears in the tubular epithelium in the medullary region (21), whereas BMP-7 expression is confined to the condensed mesenchyme and peripheral ureteric epithelium (42). Therefore, the expression pattern of USAG-1 in the developing kidney is totally different from that of BMP-7. Second, the expression of USAG-1 is very low in early embryogenesis, increases toward the late stage of embryogenesis, and is much higher in the adult kidney (21), while the expression of gremlin is high in early embryogenesis with a pattern similar to that of BMP-7, and becomes almost undetectable in the healthy adult kidney (Figure 6). Furthermore, *gremlin*-deficient mice show severe developmental abnormality in the kidney, which is quite similar to that of *BMP-7*–deficient mice. Therefore, we conclude that gremlin is a regulator of BMP-7 activity in the developing kidney, and lack of USAG-1 might be compensated by gremlin and does not cause any developmental abnormality in the kidney.

Recently another function of USAG-1 as a modulator of Wnt signaling has been reported in *Xenopus* embryogenesis (44). Although the role of the Wnt pathway in the progression of renal diseases remains to be elucidated, there is a possibility that modulation of the Wnt pathway might also play some roles in the preservation of renal function in *USAG1*$^{-/-}$ mice. Close relationships between the Wnt and BMP pathways have also been reported; for instance, dickkopf homolog 1 (DKK1), a Wnt antagonist, and noggin, a BMP antagonist, cooperate in head induction, while the expression of

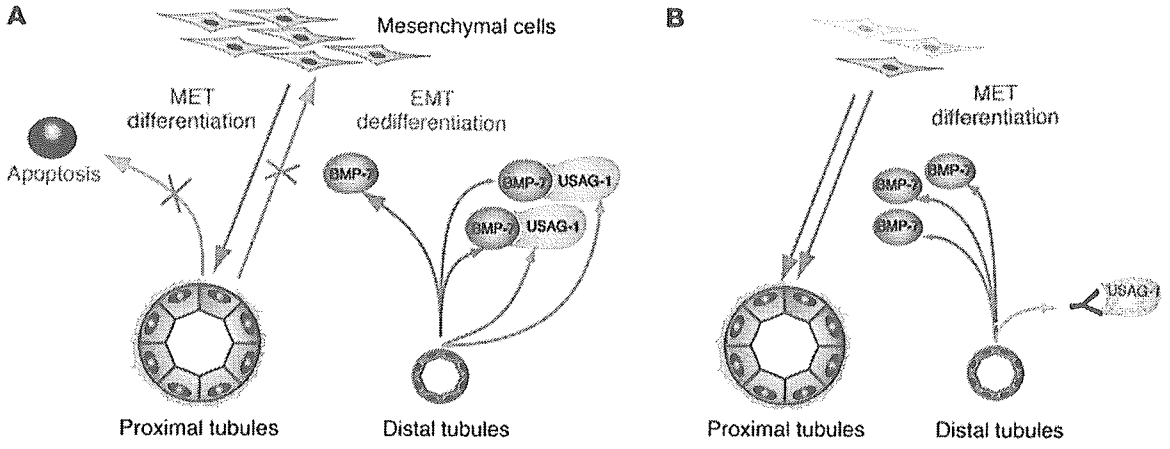

Figure 7
Working model of role of BMP-7 and USAG-1 in renal diseases. (**A**) In renal injury, PTECs are mainly damaged and undergo EMT to fibroblast-like mesenchymal cells. BMP-7 secreted by the distal tubule inhibits EMT and apoptosis of PTECs. USAG-1 is also secreted by the distal tubule, binds to BMP-7, and inhibits the renoprotective actions of BMP-7. (**B**) Therapeutic implication of USAG-1. Reduction of USAG-1 activity, for example, by a neutralizing antibody blocking the binding of USAG-1 and BMP-7, results in reinforcement of the renoprotective action of BMP-7. MET, mesenchymal-epithelial transition.

DKK1 is regulated by BMP-4 in limb development. Furthermore, a BMP antagonist, cerberus, has binding sites for both Wnt and BMP and antagonizes the activities of both the Wnt and BMP signaling pathways. USAG-1 might also have dual activities and act as a molecular link between these 2 important signaling pathways.

In conclusion, this study showed that USAG-1 plays important roles in the progression of renal diseases and might be a potent negative regulator of the renoprotective action of endogenous BMP signaling. Recently, Lin et al. identified a positive regulator of BMP-7 named kielin/chordin-like protein (KCP) and demonstrated that *KCP*$^{-/-}$ mice are susceptible to tubular injury and interstitial fibrosis (45). These data support the idea that BMP-7 protects the kidney from renal injury. Because these negative and positive modulators of BMP signaling regulate and edge the boundaries of BMP activity, further understanding of these modulators would give valuable information about their pathophysiological functions and provide a rationale for a therapeutic approach against these proteins.

Methods

Generation of USAG1$^{-/-}$ *mice.* We isolated a genomic fragment containing the mouse *USAG1* gene by screening a 129/SvJ genomic library (Stratagene). We inserted an n*lacZ* gene and a PGK-*Neo*R cassette in the opposite transcriptional orientation to the *USAG1* gene. ES cells were transfected with the linearized targeting vector by electroporation and selected by G418-containing medium. Homologous recombinants were screened and identified by genomic Southern blot analysis with an *Hinc*II-*Eco*RI probe mapping outside the 5′ homology arm (Figure 1A). Homologous recombined ES cell clones were obtained, and correct recombination was confirmed by Southern blot (Figure 1B) as well as PCR analyses. ES cells carrying the *USAG1*-null allele were injected into C57BL/6 blastocysts to obtain chimeric mice, which were crossed with wild-type C57BL/6J mice. Following germline transmission, the mice were maintained in a mixed SvJ background. PCR genotyping was used for all subsequent studies to allow specific detection of both the wild-type and *USAG1*$^{-/-}$ alleles (Figure 1C). Sequences of the primers used for genotyping are as follows: F1, CCCCTCCTCATCTGGCTGCTTCCTAAACGG; R1, CAGTCACGACGTTGTAAAACGACGGGATCC; F2, GGGATCCCACCCCTTCTCT; and R2, GCCGGGACAGGTTTAACCA.

Animal use. All experiments except those represented in Supplemental Figure 3 were performed using *USAG1*$^{-/-}$ mice and their wild-type littermates (*USAG1*$^{+/+}$) of the F_2 generation. All mice were housed in specific pathogen-

Table 1
Primers for real-time RT-PCR

Gene	Sequence of primers (5′-3′)
GAPDH	CCAGAACATCATCCCTGCATC; CCTGCTTCACCACCTTCTTGA
TNFα	ATGAGAAGTTCCCAAATGGCC; CCTCCACTTGGTGGTTTGCTA
IL-1β	CCTTCCAGGATGAGGACATGA; AACGTCACACACCAGCAGGTT
TGFβ1	GCAACAATTCCTGGCGTTACC; CGAAAGCCCTGTATTCCGTCT
MCP-1	TGCATCTGCCCTAAGGTCTTC; AAGTGCTTGAGGTGGTTGTGG
Col4α1	TTCCTTCGTGATGCACACCA; TTCTCATGCACACTTGGCAGC
USAG1	GCAACAGCACCCTGAATCAAG; TGTATTTGGTGGACCGCAGTT
Chordin	GCAGTGGTTCCCAGAGAATCA; AACAATCGTCCCGCTCACAGT
DAN	CTTCAGTTACAGCGTCCCCAA; CCAAGGTCACAATCTCCCACA
PRDC	AGGAGGCTTCCATCTCGTCAT; CCGGTTCTTCCGTGTTTCA
Twisted gastrulation	AAACGTGTCTGTTCCCAGCAA; ACACTGGTGGATGGACATGCA
Gremlin	AGCCCAAGAAGTTCACCACCA; TATGCAACGGCACTGCTTCAC
Sclerostin	CAAGCCTTCAGGAATGATGCC; TCGGACACATCTTTGGCGT
Noggin	AGAAACAGCGCCTGAGCAAGA; AAAAGCGGCTGCCTAGGTCAT
Cerberus	CCCATCAAAAGCCACGAAGT; CCAAAGCAAAGGTTGTTCTGG
Coco	TCCGCTTTTAGCCACTAGGTG; GCTGTTATTCTGGTGTCCCCA
BMP-2	TCGACCATGGTGGCCGGGACCCG; TGTTCCCGGAAGATCTGGAGT
BMP-3	AGCGAATGGATTATCTCTCCCA; TCTTTTCCGGCACACAGCA
BMP-4	CTGGAATGATTGGATTGTGGC; GCATGGTTGGTTGAGTTGAGG
BMP-5	AAGCCTGCAAGAAGCACGAA; GGAAAAGAACATTCCCCGTCA
BMP-6	CCAACCACGCCATTGTACAGA; GGAATCCAAGGCAGAACCATG
BMP-7	TGTGGCAGAAAACAGCAGCA; TCAGGTGCAATGATCCAGTCC

free conditions. Experiments represented in Supplemental Figure 3 were performed using C57BL/6 mice. All animal experiments were approved by the Animal Research Committee at the Graduate School of Medicine, Kyoto University, and the Animal Experiment and Use Committee at the University of Tsukuba and were in accordance with NIH guidelines.

Cisplatin administration. Cisplatin (Sigma-Aldrich) was administered at 20 mg/kg to mice by a single intraperitoneal injection. Mice were sacrificed 72 hours after administration of cisplatin, and tissue and blood were collected for further analysis.

UUO. Complete UUO was performed as previously described (46). Briefly, under sodium pentobarbital anesthesia, the middle portion of the left ureter was ligated and cut between 2 ligated points. At 14 days after surgery, the mice were sacrificed, and the obstructed kidneys were subjected to the studies described below.

Histological studies. The kidneys were fixed in Carnoy solution and embedded in paraffin. Sections (2 μm) were stained with PAS for routine histological examination, and the degree of morphological changes was determined using light microscopy. The following parameters were chosen as indicative of morphological damage to the kidney after cisplatin injection and UUO: brush border loss, tubule dilatation, tubule degeneration, and tubule necrosis. These parameters were evaluated on a scale of 0 to 4, and classed as: 0, not present; 1, mild; 2, moderate; 3, severe; and 4, very severe. The remaining kidney was used for immunohistochemical study, RNA isolation, and protein extraction.

Immunostaining. Frozen sections of kidneys were subjected to immunostaining with polyclonal antibodies against type IV collagen (ICN Pharmaceuticals), phosphorylated Smad1/5/8 (Cell Signaling Technology), and phosphorylated Smad2/3 (Santa Cruz Biotechnology Inc.) and monoclonal antibodies against α-SMA (Sigma-Aldrich) and Mac-1 (BD Biosciences — Pharmingen) as previously described (47, 48).

Immunoblotting. Whole kidney protein was homogenized in RIPA buffer (50 mM Tris at pH 7.5, 150 mM NaCl, 1% Nonidet P-40, 0.25% SDS, 1 mM Na_3VO_4, 2 mM EDTA, 1 mM PMSF, and 10 μg/ml aprotinin) and subjected to immunoblotting as described previously (49). Anti-E-cadherin antibody and anti-GAPDH antibody were from BD Biosciences — Transduction Laboratories and Research Diagnostic Inc., respectively.

Apoptosis detection and quantification. The TUNEL technique (In Situ Cell Death Detection Kit; Roche Diagnostics GmbH) was used to detect apoptotic cells in situ. All apoptotic nuclei within a transverse section at the renal pelvis were counted.

Quantification of mRNA by real-time RT-PCR. Real-time RT-PCR was performed with a 7700 Sequence Detection System (Applied Biosystems). Five micrograms of total RNA was reverse transcribed in a reaction volume of 20 μl using Superscript III reverse transcriptase and random primers (Invitrogen Corp.). The product was diluted to a volume of 400 μl, and 5-μl aliquots were used as templates for amplification using SYBR Green PCR amplification reagent (Applied Biosystems) and gene-specific primers. Specific primers for each gene transcript (listed in Table 1) were designed using Primer Express software version 2.0.0 (Applied Biosystems) and checked as to whether they showed a single peak in the dissociation curve. Serially diluted cDNA or plasmids encoding probes for in situ hybridization were used to generate the standard curve for each primer, and the PCR conditions were as follows: 50°C for 2 minutes, 95°C for 10 minutes, then 95°C for 15 seconds and 60°C for 1 minute for 40 cycles.

Administration of neutralizing antibody against BMP-7. In cisplatin nephrotoxicity, 1.5 mg/kg neutralizing anti–BMP-7 antibody (R&D Systems Inc.) was peritoneally injected into *USAG1*$^{-/-}$ mice 24 hours after injection of cisplatin. In UUO, 0.5 mg/kg neutralizing anti–BMP-7 antibody was injected every 3 days from day 2 to day 11. As a negative control, isotype-matched IgG2B (BD Biosciences) was injected at the same time points. Neutralizing activity of the antibody was evaluated by an assay measuring the production of alkaline phosphatase activity by C2C12 cells, as previously described (21).

In situ hybridization. The kidneys were excised from adult male mice and fixed in 4% paraformaldehyde in PBS. Frozen sections (5 μm thick) were treated with 1 μg/ml proteinase K in PBS at 37°C for 30 minutes and acetylated in 0.1 M triethanolamine-HCl, 0.25% acetic anhydride for 15 minutes. Hybridization was performed with probes at concentrations of about 1 μg/ml in a hybridization solution (50% formamide, ×5 SSC, 1% SDS, 50 μg/ml transfer RNA, and 50 μg/ml heparin) at 60°C for 16 hours. RNA probes were synthesized by in vitro transcription with a DIG RNA Labeling Mix (Roche Diagnostics Corp.). Each probe was designed to contain an open reading frame with the following length and G+C content: USAG-1, 1.0 kbp (G+C 52.6%); sclerostin, 1.5 kbp (61.7%); coco, 1.2 kbp (54.7%); DAN, 1.0 kbp (60.6%); twisted gastrulation, 0.7 kbp (55.1%); PRDC, 0.8 kbp (57.7%); chordin, 1.5 kbp (60.2%); gremlin, 0.9 kbp (50%); noggin, 0.7 kbp (64.7%); cerberus, 1.5 kbp (48.8%). Hybridization was detected using an anti-DIG AP conjugate (Roche Diagnostic Corp.) and NBT/BCIP solution (Roche Diagnostics Corp.).

Analysis of phenotype of adult teeth. Skeletal preparations of the maxillae and mandibles were made by soaking the mouse heads in 0.02% proteinase K in PBS at 37°C for 4 days after peeling off the skin, dissecting the maxillae and mandibles, and clearing them in 5% H_2O_2 at room temperature for 5 minutes. Finally they were rinsed in H_2O and left to dry.

Statistics. All assays were performed in triplicate. Data are presented as mean ± SD. Statistical significance was assessed by ANOVA, followed by Fisher's protected least significant difference post-hoc test. Survival curves were derived using the Kaplan-Meier method and compared using log-rank test.

Acknowledgments

We are grateful to Y. Nabeshima, T. Nakahata, and T. Nakamura for helpful discussion. We are grateful to M. Yoshimoto for hematological evaluation of the mice. We thank A. Godo, H. Uchiyama, and A. Hosoya for technical assistance. We thank W. Gray for reading the manuscript.

Received for publication April 25, 2005, and accepted in revised form October 11, 2005.

Address correspondence to: Motoko Yanagita, COE Formation for Genomic Analysis of Disease Model Animals with Multiple Genetic Alterations, Graduate School of Medicine, Kyoto University, Shogoin Kawahara-cho 54, Kyoto 606-8507, Japan. Phone: 81-75-751-3465; Fax: 81-75-751-3574; E-mail: motoy@kuhp.kyoto-u.ac.jp.

1. Eddy, A.A. 1996. Molecular insights into renal interstitial fibrosis. *J. Am. Soc. Nephrol.* **7**:2495–2508.
2. van Kooten, C., Daha, M.R., and van Es, L.A. 1999. Tubular epithelial cells: a critical cell type in the regulation of renal inflammatory processes. *Exp. Nephrol.* **7**:429–437.
3. Neilson, E.G. 2005. Setting a trap for tissue fibrosis. *Nat. Med.* **11**:373–374.
4. Zeisberg, M., et al. 2003. BMP-7 counteracts TGF-beta1-induced epithelial-to-mesenchymal transition and reverses chronic renal injury. *Nat. Med.* **9**:964–968.
5. Vukicevic, S., et al. 1998. Osteogenic protein-1 (bone morphogenetic protein-7) reduces severity of injury after ischemic acute renal failure in rat. *J. Clin. Invest.* **102**:202–214.
6. Hruska, K.A., et al. 2000. Osteogenic protein-1 prevents renal fibrogenesis associated with ureteral obstruction. *Am. J. Physiol. Renal. Physiol.* **279**:F130–F143.
7. Hruska, K.A. 2002. Treatment of chronic tubulointerstitial disease: a new concept. *Kidney Int.* **61**:1911–1922.
8. Zeisberg, M., et al. 2003. Bone morphogenic protein-7 inhibits progression of chronic renal fibrosis associated with two genetic mouse models. *Am. J. Physiol. Renal. Physiol.* **285**:F1060–F1067.

9. Dudley, A.T., Lyons, K.M., and Robertson, E.J. 1995. A requirement for bone morphogenetic protein-7 during development of the mammalian kidney and eye. *Genes Dev.* **9**:2795–2807.
10. Luo, G., et al. 1995. BMP-7 is an inducer of nephrogenesis, and is also required for eye development and skeletal patterning. *Genes Dev.* **9**:2808–2820.
11. Ozkaynak, E., et al. 1990. OP-1 cDNA encodes an osteogenic protein in the TGF-beta family. *EMBO J.* **9**:2085–2093.
12. Gould, S.E., Day, M., Jones, S.S., and Dorai, H. 2002. BMP-7 regulates chemokine, cytokine, and hemodynamic gene expression in proximal tubule cells. *Kidney Int.* **61**:51–60.
13. Simon, M., et al. 1999. Expression of bone morphogenetic protein-7 mRNA in normal and ischemic adult rat kidney. *Am. J. Physiol.* **276**:F382–F389.
14. Wang, S.N., Lapage, J., and Hirschberg, R. 2001. Loss of tubular bone morphogenetic protein-7 in diabetic nephropathy. *J. Am. Soc. Nephrol.* **12**:2392–2399.
15. Lund, R.J., Davies, M.R., and Hruska, K.A. 2002. Bone morphogenetic protein-7: an anti-fibrotic morphogenetic protein with therapeutic importance in renal disease. *Curr. Opin. Nephrol. Hypertens.* **11**:31–36.
16. Almanzar, M.M., et al. 1998. Osteogenic protein-1 mRNA expression is selectively modulated after acute ischemic renal injury. *J. Am. Soc. Nephrol.* **9**:1456–1463.
17. Massague, J., and Chen, Y.G. 2000. Controlling TGF-beta signaling. *Genes Dev.* **14**:627–644.
18. Simmons, D.G., and Kennedy, T.G. 2002. Uterine sensitization-associated gene-1: a novel gene induced within the rat endometrium at the time of uterine receptivity/sensitization for the decidual cell reaction. *Biol. Reprod.* **67**:1638–1645.
19. Avsian-Kretchmer, O., and Hsueh, A.J. 2004. Comparative genomic analysis of the eight-membered ring cystine knot-containing bone morphogenetic protein antagonists. *Mol. Endocrinol.* **18**:1–12.
20. Laurikkala, J., Kassai, Y., Pakkasjarvi, L., Thesleff, I., and Itoh, N. 2003. Identification of a secreted BMP antagonist, ectodin, integrating BMP, FGF, and SHH signals from the tooth enamel knot. *Dev. Biol.* **264**:91–105.
21. Yanagita, M., et al. 2004. USAG1: a bone morphogenetic protein antagonist abundantly expressed in the kidney. *Biochem. Biophys. Res. Commun.* **316**:490–500.
22. Schrier, R.W. 2002. Cancer therapy and renal injury. *J. Clin. Invest.* **110**:743–745. doi:10.1172/JCI200216568.
23. Megyesi, J., Safirstein, R.L., and Price, P.M. 1998. Induction of p21WAF1/CIP1/SDI1 in kidney tubule cells affects the course of cisplatin-induced acute renal failure. *J. Clin. Invest.* **101**:777–782.
24. Ramesh, G., and Reeves, W.B. 2002. TNF-α mediates chemokine and cytokine expression and renal injury in cisplatin nephrotoxicity. *J. Clin. Invest.* **110**:835–842. doi:10.1172/JCI200215606.
25. Yang, J., and Liu, Y. 2001. Dissection of key events in tubular epithelial to myofibroblast transition and its implications in renal interstitial fibrosis. *Am. J. Pathol.* **159**:1465–1475.
26. Klahr, S., and Morrissey, J. 2002. Obstructive nephropathy and renal fibrosis. *Am. J. Physiol. Renal. Physiol.* **283**:F861–F875.
27. Chevalier, R.L. 1999. Molecular and cellular pathophysiology of obstructive nephropathy. *Pediatr. Nephrol.* **13**:612–619.
28. Sato, M., Muragaki, Y., Saika, S., Roberts, A.B., and Ooshima, A. 2003. Targeted disruption of TGF-beta1/Smad3 signaling protects against renal tubulointerstitial fibrosis induced by unilateral ureteral obstruction. *J. Clin. Invest.* **112**:1486–1494. doi:10.1172/JCI200319270.
29. Kalluri, R., and Neilson, E.G. 2003. Epithelial-mesenchymal transition and its implications for fibrosis. *J. Clin. Invest.* **112**:1776–1784. doi:10.1172/JCI200320530.
30. Bottinger, E.P., and Bitzer, M. 2002. TGF-beta signaling in renal disease. *J. Am. Soc. Nephrol.* **13**:2600–2610.
31. Iwano, M., et al. 2002. Evidence that fibroblasts derive from epithelium during tissue fibrosis. *J. Clin. Invest.* **110**:341–350. doi:10.1172/JCI200215518.
32. Zeisberg, M., Shah, A.A., and Kalluri, R. 2005. Bone morphogenic protein-7 induces mesenchymal to epithelial transition in adult renal fibroblasts and facilitates regeneration of injured kidney. *J. Biol. Chem.* **280**:8094–8100.
33. Gerritsma, J.S., van Kooten, C., Gerritsen, A.F., van Es, L.A., and Daha, M.R. 1998. Transforming growth factor-beta 1 regulates chemokine and complement production by human proximal tubular epithelial cells. *Kidney Int.* **53**:609–616.
34. Li, T., Surendran, K., Zawaideh, M.A., Mathew, S., and Hruska, K.A. 2004. Bone morphogenetic protein 7: a novel treatment for chronic renal and bone disease. *Curr. Opin. Nephrol. Hypertens.* **13**:417–422.
35. Davies, M.R., Lund, R.J., Mathew, S., and Hruska, K.A. 2005. Low turnover osteodystrophy and vascular calcification are amenable to skeletal anabolism in an animal model of chronic kidney disease and the metabolic syndrome. *J. Am. Soc. Nephrol.* **16**:917–928.
36. Gonzalez, E.A., et al. 2002. Treatment of a murine model of high-turnover renal osteodystrophy by exogenous BMP-7. *Kidney Int.* **61**:1322–1331.
37. Hruska, K.A., et al. 2004. Kidney-bone, bone-kidney, and cell-cell communications in renal osteodystrophy. *Semin. Nephrol.* **24**:25–38.
38. Lund, R.J., Davies, M.R., Brown, A.J., and Hruska, K.A. 2004. Successful treatment of an adynamic bone disorder with bone morphogenetic protein-7 in a renal ablation model. *J. Am. Soc. Nephrol.* **15**:359–369.
39. Simic, P., and Vukicevic, S. 2005. Bone morphogenetic proteins in development and homeostasis of kidney. *Cytokine Growth Factor Rev.* **16**:299–308.
40. Davies, M.R., Lund, R.J., and Hruska, K.A. 2003. BMP-7 is an efficacious treatment of vascular calcification in a murine model of atherosclerosis and chronic renal failure. *J. Am. Soc. Nephrol.* **14**:1559–1567.
41. Hruska, K.A., Mathew, S., and Saab, G. 2005. Bone morphogenetic proteins in vascular calcification. *Circ. Res.* **97**:105–114.
42. Godin, R.E., Takaesu, N.T., Robertson, E.J., and Dudley, A.T. 1998. Regulation of BMP7 expression during kidney development. *Development.* **125**:3473–3482.
43. Michos, O., et al. 2004. Gremlin-mediated BMP antagonism induces the epithelial-mesenchymal feedback signaling controlling metanephric kidney and limb organogenesis. *Development.* **131**:3401–3410.
44. Itasaki, N., et al. 2003. Wise, a context-dependent activator and inhibitor of Wnt signalling. *Development.* **130**:4295–4305.
45. Lin, J., et al. 2005. Kielin/chordin-like protein, a novel enhancer of BMP signaling, attenuates renal fibrotic disease. *Nat. Med.* **11**:387–393.
46. Nishida, M., et al. 2002. Absence of angiotensin II type 1 receptor in bone marrow-derived cells is detrimental in the evolution of renal fibrosis. *J. Clin. Invest.* **110**:1859–1868. doi:10.1172/JCI200215045.
47. Yanagita, M., et al. 2001. Gas6 regulates mesangial cell proliferation through Axl in experimental glomerulonephritis. *Am. J. Pathol.* **158**:1423–1432.
48. Yanagita, M., et al. 2001. Gas6 induces mesangial cell proliferation via latent transcription factor STAT3. *J. Biol. Chem.* **276**:42364–42369.
49. Yanagita, M., et al. 2002. Essential role of Gas6 for glomerular injury in nephrotoxic nephritis. *J. Clin. Invest.* **110**:239–246. doi:10.1172/JCI200214861.